CHAPTER 3

RESULTS AND DISCUSSION

The results of this study were divided into 4 parts according to the following methods:

Part 1: Collection of the plants

Part 1: Preparation of the crude extracts and bioactivity screening tests

Part 2: Extraction, isolation, purification and structure elucidation of the selected plants

Part 3: Bioactivities of the isolated compounds

Part 1: Collection of the plants

According to review the literature both of the chemical constituents and biological acitivities of plant species from Guttiferae and Schisandraceae families and also study the name list of plant species which were authenticated and deposited at the herbarium, Faculty of Science and Faculty of Pharmacy, Chiang Mai University, leaves, stem wood of five plants from the Guttiferae (*Hypericum hookerianum*, *Garcinia speciosa*, *Garcinia xanthochymus*, *Cratoxylum formosum* ssp. *pruniflorum*, *Calophyllum polyanthum*), the one from Schisandraceae (*Schisandra verruculosa*) and the fruit of *G. xanthochymus* which were collected from the mountain in Chiang Mai province, were selected to screen for the free radical scavenging activity by the DPPH assay and antitumor activity by the SRB assay. These activities have never been previous reported from all of the selected plants.

Part 2 : Preparation of the crude extracts and bioactivity screening tests

2.1 Preparation of the crude extracts

The percentage yields and moisture contents of the methanol and chloroform fraction of the methanol extracts from different parts of each plant were shown in Table 3.1 (the calculation data are in appendix A). Methanol extracts of all plants showed higher percentage yield than the chloroform-fractioned methanol extracts. This might be due to the presence of more polar compounds in the plants which are more soluble in methanol than in chloroform.

Table 3.1 The percentage yields and moisture contents of methanol and chloroform fraction of the methanol extracts from various parts of the selected Thai plants in family Guttiferrae and Schisandraceae.

		Yield (%)					
		Wood		Leaf		Fruit	
Plants	Moisture content (%)	MeOH	$CHCl_3$	MeOH	$CHCl_3$	MeOH	$CHCl_3$
Guttiferae							
H. hookerianum	8.65	7.36	2.01	ND	ND	ND	ND
G. speciosa	39.90	12.18	0.66	8.61	4.33	ND	ND
G. xanthochymus	41.80	19.04	1.02	12.45	1.67	23.60	9.69
C. formosum ssp. *pruniflorum*	38.39	3.77	1.01	14.60	4.50	ND	ND
C. polyanthum	48.18	4.46	2.65	11.10	8.50	ND	ND
Schisandraceae							
S. verruculosa	31.61	1.77	1.22	4.14	3.94	ND	ND

Note: MeOH = methanol extract; $CHCl_3$ = chloroform fraction of the methanol extract; ND = not determined

2.2 Free radical scavenging activity study of crude extracts (DPPH assay)

For scavenging activity, hydrogen donating ability of the extract to the free radical (DPPH) was determined. When DPPH is scavenged, the deep violet color turns to pale yellow which can be determined spectrophotometrically. All extracts showed scavenging activity in a concentration dependent pattern (Figure 3.1 – 3.4).

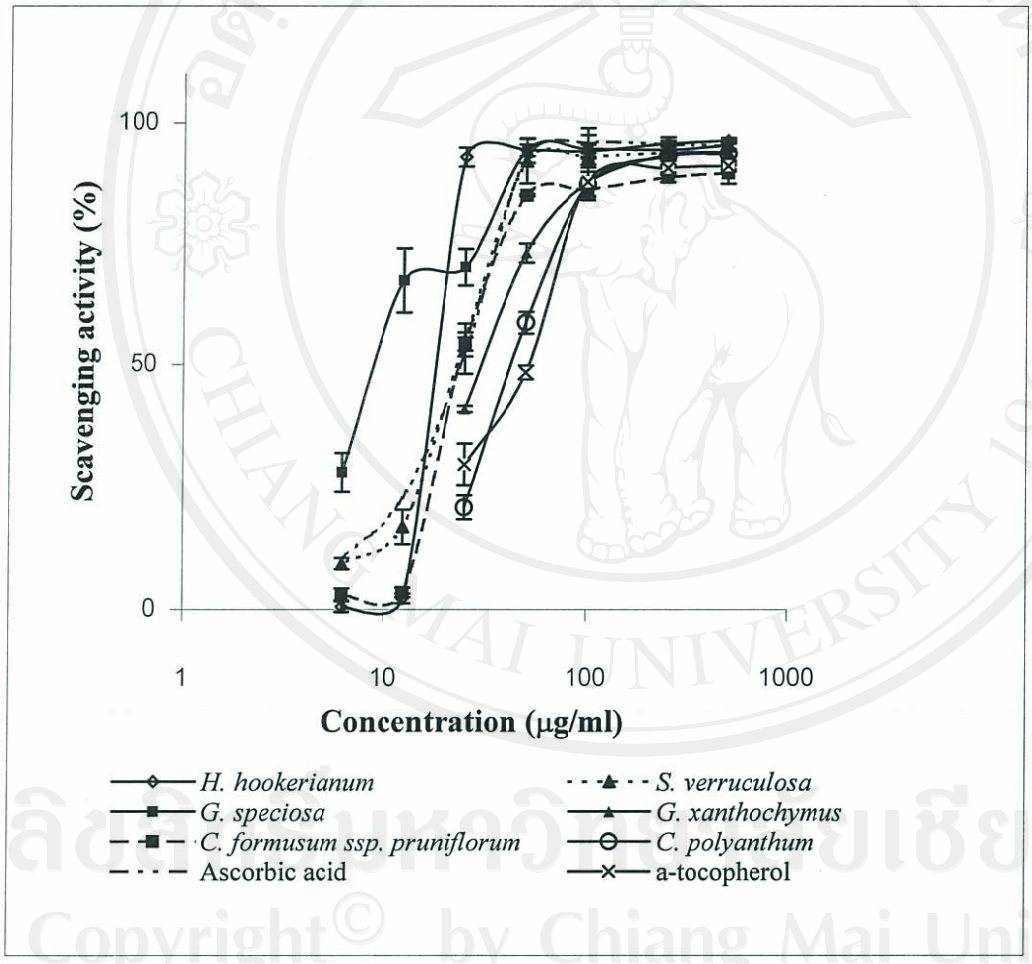

Figure 3.1 Comparison of free radical scavenging activity (%) of the methanol wood extracts of the six selected Thai plants with the standard antioxidants. Vertical bars represent the standard deviation of three replicates.

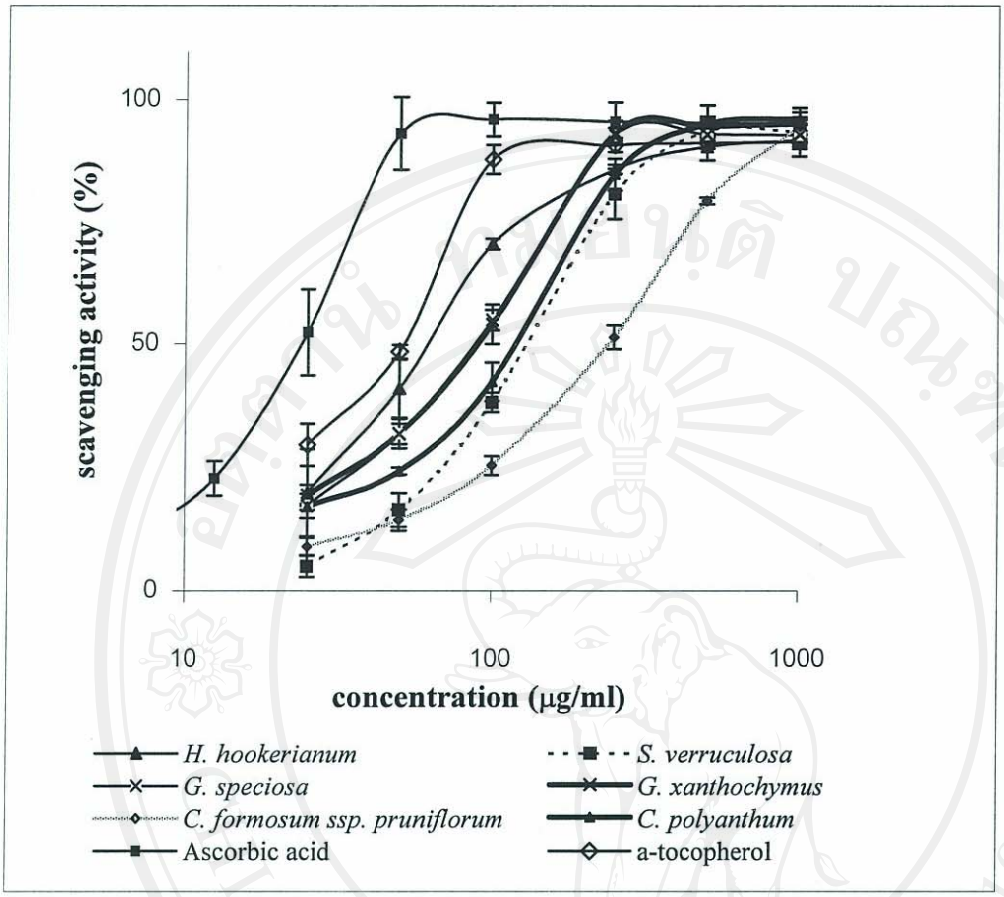

Figure 3.2 Comparison of free radical scavenging activity of the chloroform fraction of the methanol wood extracts of the six selected Thai plants with the standard antioxidants. Vertical bars represent the standard deviation of three replicates.

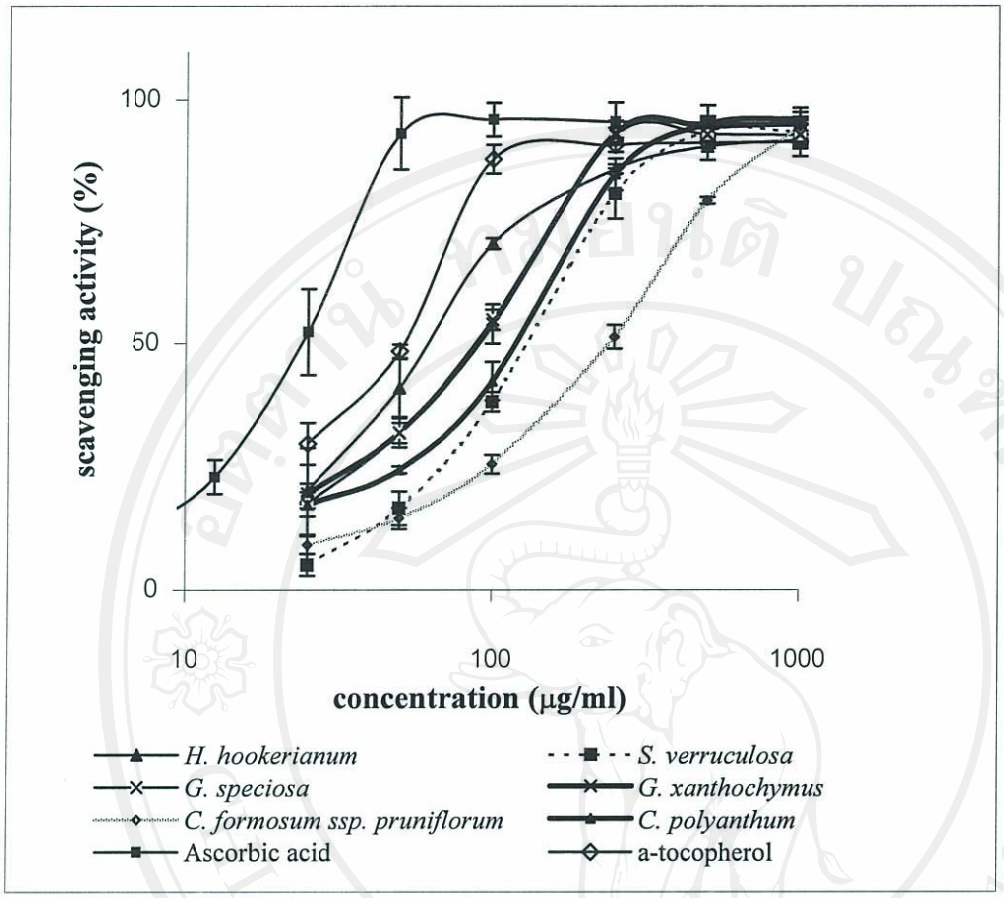

Figure 3.3 Comparison of free radical scavenging activity (%) of the methanol leaves extracts of the six selected Thai plants with the standard antioxidants. Vertical bars represent the standard deviation of three replicates.

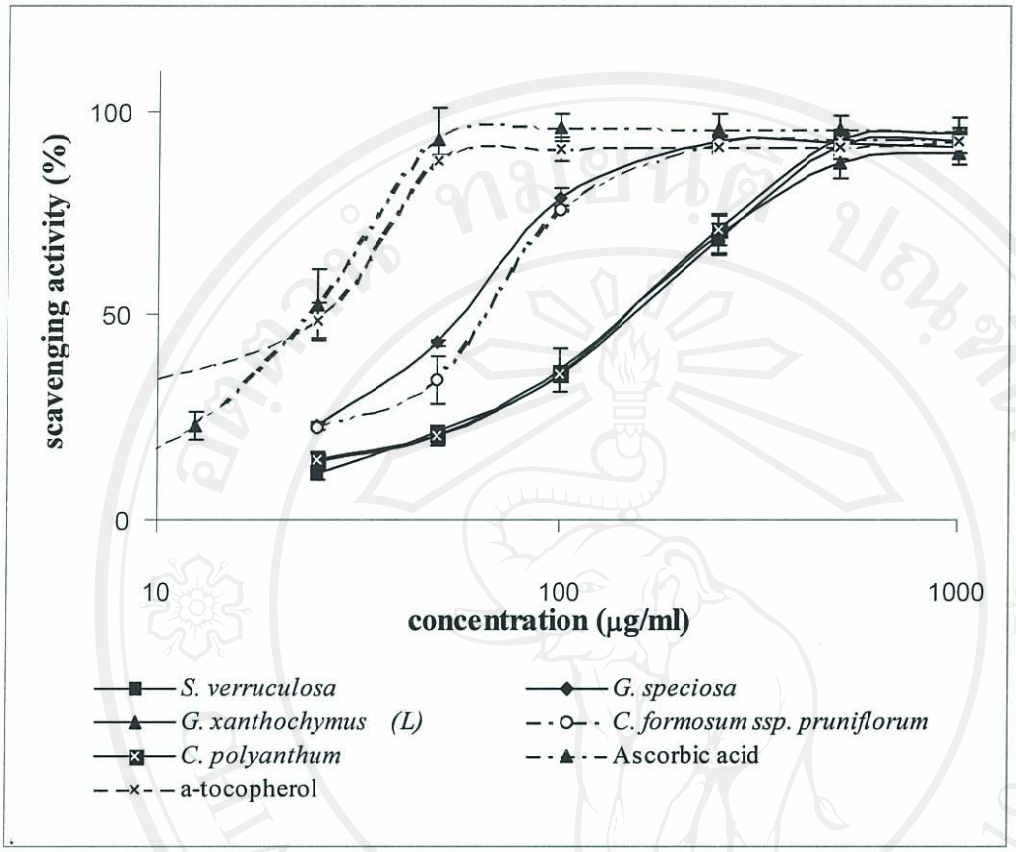

Figure 3.4 Comparison of free radical scavenging activity (%) of the chloroform fraction of the methanol leaves extracts of the six selected Thai plants with the standard antioxidants. Vertical bars represent the standard deviation of three replicates.

Table 3.2 The IC_{50} values of the selected Thai plant extracts.

Plant species	IC_{50} (μg/ml)					
	Wood		Leaf		Fruit	
	MeOH	$CHCl_3$	MeOH	$CHCl_3$	MeOH	$CHCl_3$
Guttiferae						
H. hookerianum	19.08	65.42	-	-	-	-
G. speciosa	9.75	142	65.13	168	-	-
G. xanthochymus	32.10	89.56	58.69	59.83	25.58	26.68
C. formosum ssp. *pruniflorum*	23.96	91.04	93.28	162.34	-	-
C. polyanthum	44.29	242.25	51.88	69.41	-	-
Schisandraceae						
S. verruculosa	23.34	127.34	130.00	162.18	-	-

Note: MeOH = methanol extract; $CHCl_3$ = chloroform fraction of the methanol extract

IC_{50}; the concentration of extract which showed 50% DPPH scavenging activity

Table 3.2 demonstrated the IC_{50} of the extracts. All methanol extracts gave lower IC_{50} values than the chloroform fraction of the methanol extracts. These results agree with the previous study of Moure *et al.*, (2000) indicating the dependence of antioxidant activity of the plant extracts on the polarity of extracting solvents.

In comparing the extract from wood and leaf of each plant, the scavenging activity of methanol wood extract of all plants exhibited higher scavenging activity than their leaves. This might be due to the higher content of the total polyphenolic compounds in the wood than in leaves. These polyphenolic compounds include flavonoids, anthraquinones, anthocyanidins, xanthones and tannins. These

compounds have been reported to scavenge free radicals, superoxide and hydroxyl radical by single electron transfer (Choi *et al.*, 2002; Ho *et al.*, 1999). The highest scavenging activity was found in the methanol wood extract of *G. speciosa* with an IC_{50} value of 9.75 μg/ml which were 2.5 and 5.3 folds more potents than the standard antioxidant, ascorbic acid and α-tocopherol, respectively. *H. hookerianum*, S. *verruculosa, C. formosum* ssp. *pruniflorum, G. xanthochymus, and C. polyanthum* gave the IC_{50} values of 19.08, 23.34, 23.96, 32.10 and 44.29 μg/ml, respectively. In fact, some of these values were less than those obtained from standard antioxidants, ascorbic acid and α-tocopherol (the IC_{50} values of ascorbic acid and α-tocopherol were found to be 24.01 and 52.04 μg/ml respectively). For *G. xanthochymus*, the IC_{50} values of methanol and chloroform fraction of the methanol extract were not significant by differrent in fruits (25.58 and 26.68 μg/ml) and leaves (58.69 and 59.83 μg/ml). The extracts from *G. xanthochymus* using polar and non-polar solvents appeared to give equi-potency of the free radical scavenging activity.

2.3 An antitumor activity study of crude extracts (SRB assay)

The effect of extracts on the growth of human cancer cell lines using SRB assay were evaluated. The GI_{50} (the concentrations of extracts that cause 50% inhibition of cancer cell growth) of extracts on HeLa, KB and B16F10 cell lines, were shown in Table 3.3 - 3.4 (Calculation data are in appendix B). Final concentration of DMSO (≤ 0.25%) did not interfere with the biological activities tested. Extracts exhibited a dose dependent growth inhibitory effect on all the cancer cell lines and each extract gave the GI_{50} values which were not significant different in three cell lines.

Table 3.3 Effect of methanol and chloroform fraction of the methanol extracts from wood of the selected Thai plants in family Guttiferrae and Schisandraceae on the growth of human cancer cell lines.

Plant species		GI_{50} (μg/ml)		
		HeLa	KB	B16F10
Guttiferae				
H. hookerianum	M	42.3 ± 1.5	46.3 ± 1.5	51.0 ± 8.5
	C	19.7 ± 1.2	19.3 ± 1.5	14.5± 0.7
G. speciosa	M	67.3 ± 2.5	75.0 ± 0.6	82.0 ± 4.2
	C	9.9 ± 1.2	15.7 ± 0.6	8.1 ± 0.1
G. xanthochymus	M	130.0	123.3 ± 5.8	105.0 ± 7.1
	C	13.3 ± 1.5	19.0 ± 1.0	11.5 ± 0.7
C. formosum ssp. *pruniflorum*	M	> 250	193.3 ± 5.8	> 250
	C	41.3 ± 1.5	37.3 ± 0.6	44.5 ± 2.1
C. polyanthum	M	216.7 ± 5.8	156.7 ± 25.2	160.0 ± 28.3
	C	90.3 ± 3.1	74.7 ± 3.2	52.5 ± 3.5
Schisandraceae				
S. verruculosa	M	170.0 ± 10	70.7 ± 6.4	200.0 ± 14.1
	C	136.7 ± 5.7	98.0 ± 2.7	70.0 ± 1.4

Note: M = methanol extract; C = chloroform fraction of the methanol extract; ND = not determined

Results are expressed as GI_{50} that are arithmetical means ± SD of 3 independent experiments performed in duplicate.

Doxorubicin was used as positive control (GI_{50} Hela = 300 ± 0.9 nM ; GI_{50} KB = 330 ± 0.9 nM; GI_{50} B16F10 = 26 ± 0.2 nM)

Table 3.4 Effect of methanol and chloroform fraction of the methanol extracts from leaves of the selected Thai plants in family Guttiferrae and Schisandraceae on the growth of human cancer cell lines.

Plant species		GI_{50} (μg/ml)		
		HeLa	KB	B16F10
Guttiferae				
H. hookerianum	M	ND	ND	ND
	C	ND	ND	ND
G. speciosa	M	34.7 ± 2.3	23.7 ± 0.6	25.7 ± 0.6
	C	4.0 ± 0.3	6.6 ± 0.2	3.7 ± 0.4
G. xanthochymus	M	223.3 ± 11.6	116.7 ± 5.8	160.0
	C	17.0 ± 1.0	29.3 ± 0.6	37.7 ± 4.0
C. formosum ssp. *pruniflorum*	M	> 250	> 250	> 250
	C	223.3 ± 20.1	180.0 ± 10	> 250
C. polyanthum	M	> 250	> 250	> 250
	C	19.0 ± 2.7	13.3 ± 0.6	11.0 ± 1.1
Schisandraceae				
S. verruculosa	M	> 250	> 250	> 250
	C	160.0 ± 10	> 250	183.3 ± 11

Note: M = methanol extract; C = chloroform fraction of the methanol extract; ND = not determined

Results are expressed as GI_{50} that are arithmetical means ± SD of 3 independent experiments performed in duplicate.

Doxorubicin was used as positive control (GI_{50} Hela = 300 ± 0.9 nM ; GI_{50} KB = 330 ± 0.9 nM; GI_{50} B16F10 = 26 ± 0.2 nM)

The chloroform fraction of the methanol leaves extract of *G. speciosa* showed the most potent inhibitory effect with GI_{50} values of 4.0, 6.6 and 3.7 μg/ml on HeLa, KB and B16F10 cell lines, respectively. These values were 13, 20 and 142 folds less potent than doxorubicin, the positive control, which gave the GI_{50} values of 300 nM, 330 nM and 26 on HeLa, KB and B16F10 cell lines, respectively. The strong growth inhibitory effects were also detected in the chloroform fraction of the methanol leaves extract of *C. polyanthum* with GI_{50} value of 13.3, 19.0 and 11.0 μg/ml.

From the wood, the chloroform fraction of the methanol extract of *G. speciosa* also showed strong cell growth inhibition with the GI_{50} values of 9.9, 15.7 and 8.1 μg/ml on B16F10, HeLa and KB cell lines, respectively. Chloroform fraction of the methanol extracts of *H. hookerianum*, and *G. xanthochymus* were also exhibited the inhibitory effect on cell growth with GI_{50} value less than 20 μg/ml. The stronger inhibitory effects of most of the chloroform fraction of the methanol extracts comparing to the methanol extracts might be due to the presence of more active compounds, non polar compounds which are more soluble in chloroform.

Moderate inhibitory effect were found in the methanol leaves extract of *G. speciosa*, the chloroform fraction of the methanol leaves extract of *G. xanthochymus*, the chloroform fraction of the methanol wood extract of *C. formosum* ssp. *Pruniflorum* and the methanol wood extract of *H. hookerianum*. Both of the methanol and chloroform-fractioned methanol leaves extracts of *C. formosum* ssp. *Pruniflorum*, and *S. verruculosa* showed inhibitory activity with GI_{50} value more than 100 μg/ml.

The results from this study suggested a potential for the plants with significant growth inhibitory activity for possible further study and development of pure compounds in the crude extracts to new pharmaceuticals.

Part 3: Extraction, isolation, purification and structure elucidation of the selected plants

According to the screening of the biological activities of the leaves and stem wood extracts from *Hypericum hookerianum*, *Garcinia speciosa*, *Garcinia xanthochymus*, *Cratoxylum formosum* ssp. *pruniflorum, Calophyllum polyanthum* and *Schisandra verruculosa*, the results showed that *G. speciosa* gave the highest activities but its chemical constituents have already been reported (Rukachaisirikul *et al.*,2003; Viera *et al.*, 2004). *G. xanthochymus*, *C. formosum* ssp. *pruniflorum* have also been reported (Chanmahasathien et al., 2003; Nguyen & Harison, 1998).

For *H. hookerianum*, there was no report on chemical study including the screening test of antioxidant and antitumor activities. From this study, the stem wood crude extract of *H. hookerianum* showed the high activities on both of free radical scavenging activity and antitumor activity. The wood of *C. polyanthum* also gave moderate free radical scavenging and antitumor activities with no data on chemical constituents since only small amount of crude extract was obtained which was not enough for purification. The collection was very difficult because the tree was found in the valley, so only the small trees were collected. Although *S. verruculosa* showed weak to moderate activities on the free radical scavenging and antitumor activity screening test, no chemical study has been reported. Thus, *H. hookerianum* and *S. verruculosa* were selected for the study of phytochemistry and biological activities of the isolated compounds.

Diagrams of the isolation and purification of the isolated compounds from *H. hookerianum* and *S. verruculosa* are shown as follows:

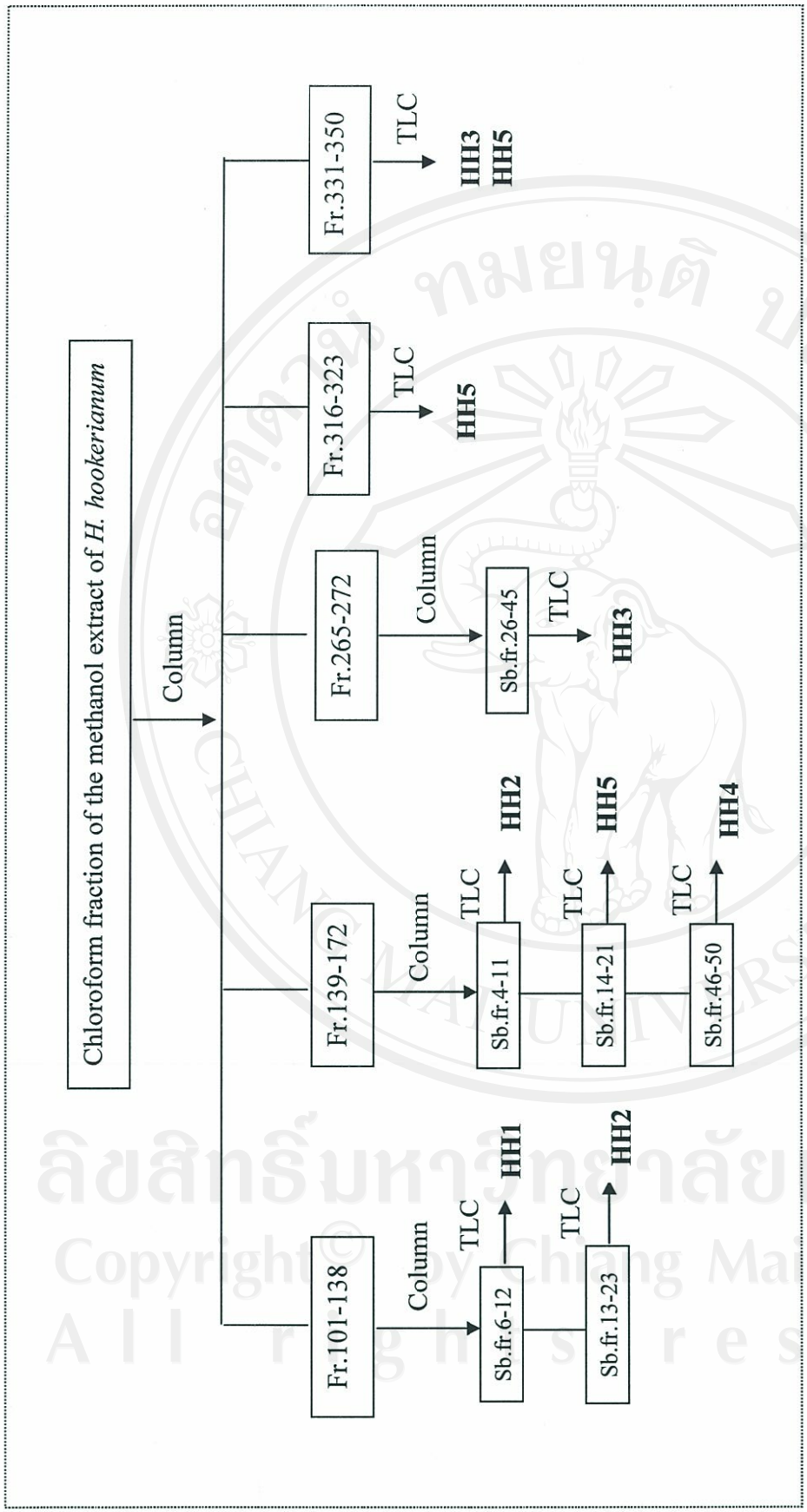

Figure 3.5 Diagram of the isolation and purification of the isolated compounds from *Hypericum hookerianum*

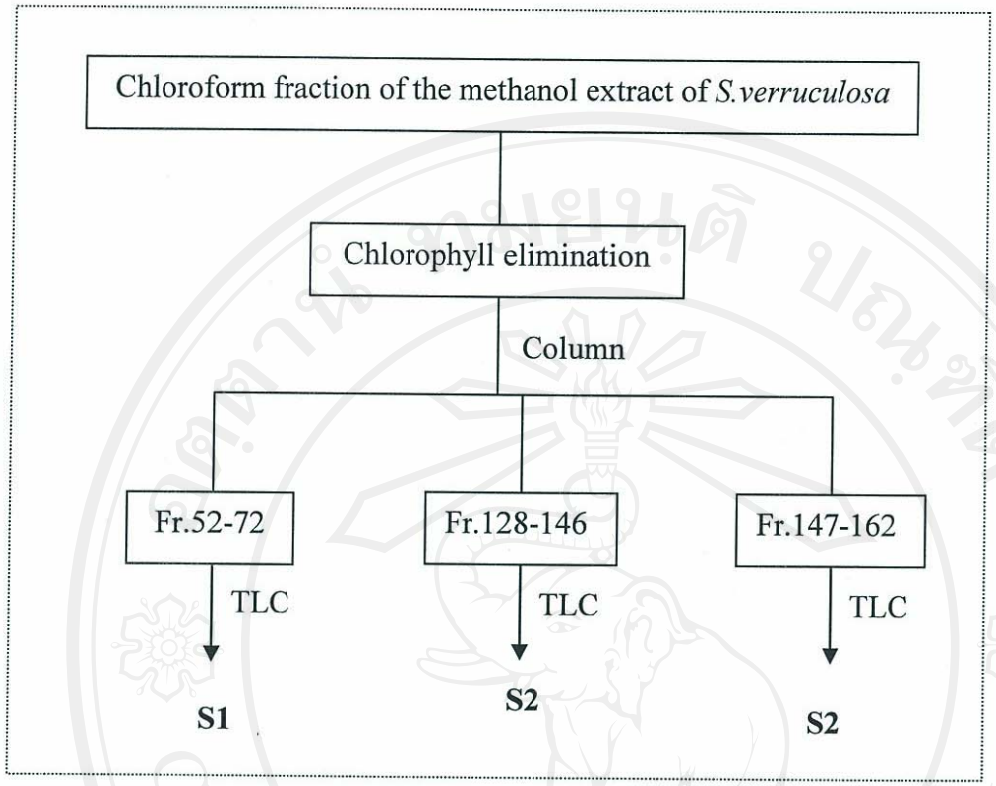

Figure 3.6 Diagram of the isolation and purification of the isolated compounds from *Schisandra verruculasa*

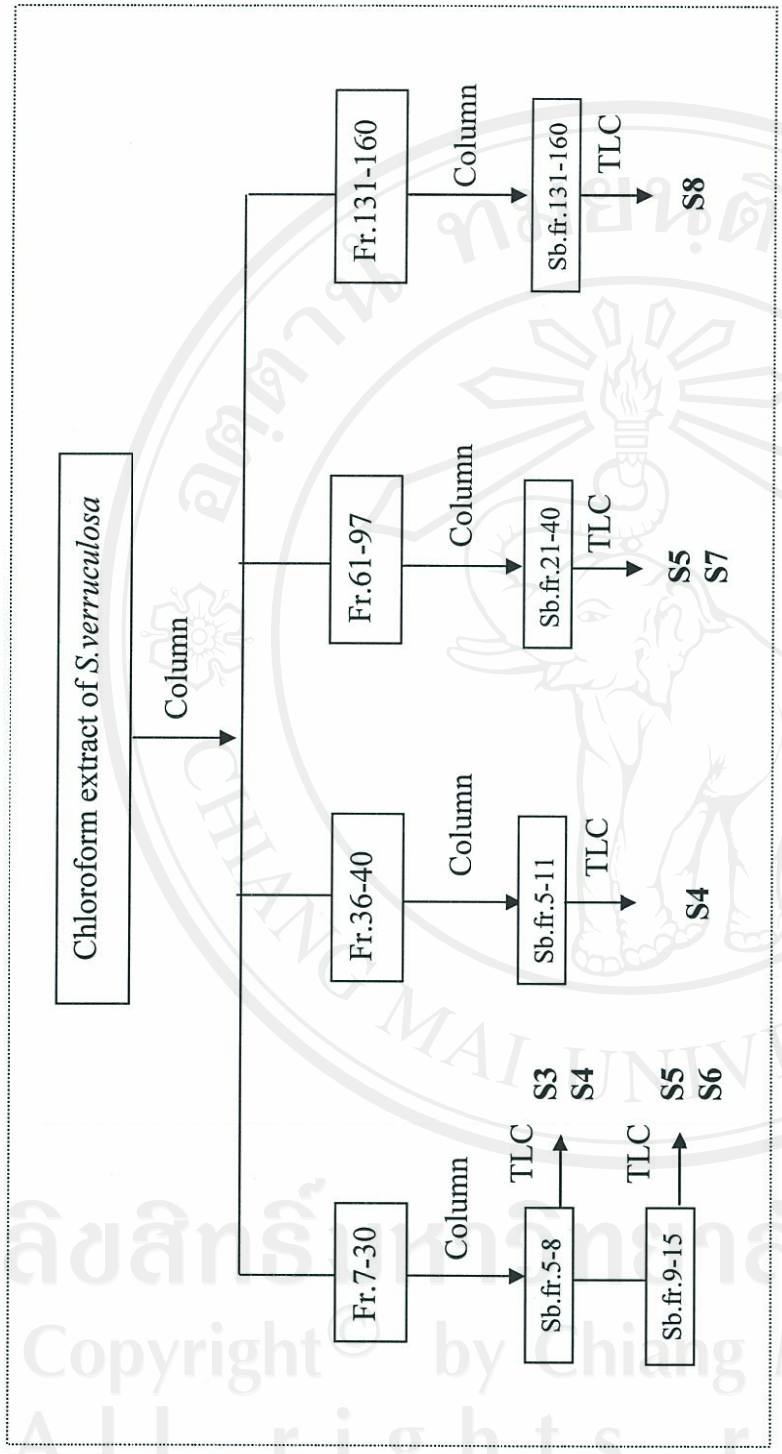

Figure 3.7 Diagram of the isolation and purification of the isolated compounds from S*chisandra verruculasa*

3.1 Extraction, isolation, purification and structure elucidation of *Hypericum hookerianum*

3.1.1 Preparation of the extract

Dried and powdered woody stems of *H. hookerianum* (5.5 kg) were percolated by MeOH (3x10 L) at room temperature. The solution was evaporated at reduced pressure and the crude residue (81g) was dissolved in $CHCl_3$ (3x500 ml) and concentrated by partial evaporation under reduced pressure to afford the crude chloroform fraction of the methanol extract (62 g).

3.1.2 Fractionation of the extract

The crude chloroform fraction of the methanol extract (62 g) was loaded on the silica gel G60 (300 g), in a column (90 x 4.5 cm), and eluted with Petrol- $CHCl_3$, $CHCl_3$,$CHCl_3$-acetone, 250 ml fractions being collected as follows.

Eluents	**Fractions**
Petrol-$CHCl_3$ (7:3)	1-133
Petrol-$CHCl_3$ (1:1)	134-263
$CHCl_3$-Petrol (4:1)	264-365
$CHCl_3$-$(CH_3)_2CO$ (9:1)	366-464
$CHCl_3$-$(CH_3)_2CO$ (7:3)	465-487

All fractions were monitored by analytical TLC and combined, according to their composition, as follows:

Fractions	**Isolated compounds**
1-29	not purified
30-34 (3.7 g)	not purified

35-40 (5.2 g)	not purified
41-45 (1.0 g)	not purified
46-54 (63.6 mg)	not purified
56-66 (90.6 mg)	not purified
67-77 (72.4 mg)	not purified
78-88 (49.6 mg)	not purified
89-100 (60.1 mg)	not purified
101-138 (1.3 g)	small column
139-172 (2.1 g)	small column
173-264 (2.4 g)	not purified
265-272 (89 mg)	small column
273-315 (2.2 g)	not purified
316-32 (100 mg)	**HH5** (10 mg)
324-330 (21.2 mg)	not purified
331-350 (556 mg)	**HH3** (52 mg), **HH5** (72 mg)
341-350 (217.8 mg)	not purified
351-360 (194.2 mg)	not purified
361-368 (131.2 mg)	not purified
369-390 (1.4 g)	not purified
391-418 (92.3 mg)	not purified
419-440 (46.9 mg)	not purified
449-466 (166.4 mg)	not purified
467-676 (39.5 mg)	not purified
477-486 (1.7 g)	not purified

3.1.3 Isolation and Purification of the Constituents

Fraction 101-138 were combined (1.3 g), placed on a silica gel column (30 g, 40 x 3cm), and eluted with Petrol-$CHCl_3$, 300 ml subfractions being collected as follows:

Eluents	**Subfractions**
Petrol- $CHCl_3$ (7:3)	1- 40
Petrol- $CHCl_3$ (1:1)	41-55

Subfractions were combined according to their composition as appeared by analytical TLC, as follows:

Subfractions	**Isolated compounds**
1-5	not purified
6-12 (163 mg)	**HH 1** (79 mg)
13-23 (87 mg)	**HH 2** (38 mg)
24-30 (55.8 mg)	not purified
31-35 (9.9 mg)	not purified
36-40 (5.9 mg)	not purified
41-48 (192.3 mg)	not purified
49-55 (12.9 mg)	not purified

Purification of subfractions 6-12 (163 mg) by preparative TLC ($CHCl_3$-Petrol-HCO_2H, 95:5:0.1) gave yellowish crystals of **HH1** (79 mg).

Subfraction 13-23 (87 mg) were combined and purified by preparative TLC ($CHCl_3$-$(CH_3)_2CO$-HCO_2H, 95:5:0.1) to give yellow needle of **HH2** (38 mg).

Fraction 139-172 (2.1 g) were combined, placed on silica gel 60 column (40 g, 2.5 x 30 cm) and eluted with Petrol- $CHCl_3$, 250 ml subfractions being collected as follows:

Eluents	**Subfractions**
Petrol- $CHCl_3$ (1:1)	1-33
$CHCl_3$-Petrol (7:3)	34-80
$CHCl_3$-Petrol (9:1)	81-95

All fractions were monitored by analytical TLC and combined, according to their composition, as follows:

Subfractions	**Isolated compounds**
1-3 (63.2 mg)	not purified
4-11 (134 mg)	**HH2** (41 mg)
12-13 (37.5 mg)	not purified
14-21 (39 mg)	**HH5** (35 mg)
22-25 (83.4 mg)	not purified
26-30 (62.8 mg)	not purified
31-34 (86.5 mg)	not purified
35-37 (317.6 mg)	not purified
38-45 (475.6 mg)	not purified
46-50 (189 mg)	**HH 4** (44 mg)
51-55 (109.9 mg)	not purified
56-60 (90 mg)	not purified
61-65 (44.7 mg)	not purified
66-70 (41.3 mg)	not purified

71-75 (72.6 mg)	not purified
76-80 (80.2 mg)	not purified
81-85 (89.3 mg)	not purified
86-90 (60.4 mg)	not purified
91-95 (56.3 mg)	not purified

Subfractions 4-11 (134 mg) were combined and purified by preparative TLC ($CHCl_3$-$(CH_3)_2CO$-HCO_2H, 9:1:0.1) to give **HH2** (41 mg).

Subfractions 14-21 (39 mg) were combined and similary purified by preparative TLC to give **HH5** (35 mg).

Purification of subfractions 46-50 (189 mg) by preparative TLC ($CHCl_3$-$(CH_3)_2CO$- HCO_2H, 8.5:1.5:0.1) afforded **HH4** (44 mg).

Fraction 265-272 were combined (89 mg) were also combined, placed on a silica gel column (15 g, 2.5 x 30 cm) and eluted with Petrol-$CHCl_3$,100 ml subfractions being collected as follows:

Eluents	**Subfractions**
Petrol- $CHCl_3$ (1:1)	1-41
$CHCl_3$-Petrol (4:1)	42-60

Subfractions were combined according to their composition as revealed by analytical TLC, as follows:

Subfractions	**Isolated compounds**
1-11 (221 mg)	not purified
12-15 (73 mg)	not purified

16-22 (111 mg)	not purified
23-25 (25 mg)	not purified
26-45 (125 mg)	**HH3** (35 mg)
46-58 (292 mg)	not purified

Purification of subfractions 26-45 (125 mg) by preparative TLC ($CHCl_3$-$(CH_3)_2CO$- HCO_2H, 9.5:0.5:0.1) afforded crystals of **HH3** (35 mg).

Fractions 316-323 (100 mg) were purified by preparative TLC ($CHCl_3$-$CH_3COOC_2H_5$-$(CH_3)_2CO$-HCO_2H, 8.5:1:0.5:0.1) to give **HH 5** (10 mg) while purification of fractions 331-350 (556 mg) by preparative TLC (Silica gel, $CHCl_3$-$(CH_3)_2CO$-HCO_2H, 9.5:0.5:0.1) afforded **HH3** (52 mg) and **HH5** (72 mg).

3.1.4 Stucture elucidation

Compounds HH1-HH5 were elucidated for their structure by ^1H-, ^{13}C-NMR, mass spectrometry, COSY, HSQC, HMBC and NOESY.

HH1 was identified as 5-hydroxy-2-methoxyxanthone (Fig. 3.7). ^1H-, ^{13}C-NMR, COSY, HSQC and HMBC spectra were shown in Table 3.5-3.8. Chemical shifts and coupling constant of HH1 was showed in Figure 3.8.

HH2 was identified as 2-hydroxy-3-methoxyxanthone (Fig. 3.9). ^1H-, ^{13}C-NMR and HMBC spectra were shown in Table 3.9-3.11. Chemical shifts and coupling constant of HH2 was showed in Figure 3.10.

HH3 was identified as *trans*-kielcorin (Fig. 3.11). ^1H-NMR, COSY, HSQC, HMBC and NOSY spectra were shown in Table 3.12-3.16. Chemical shifts and coupling constant of HH3 was showed in Figure 3.12.

HH4 was identified as 4-hydroxy-3-methoxyphenyl ferulate (Fig. 3.13). ^{1}H-, ^{13}C-NMR, COSY, HSQC and HMBC spectra were shown in Table 3.17-3.20 and chemical shifts and coupling constant of HH4 was showed in Figure 3.12.

HH5 was identified as 3β- O-caffeoylbetulinic acid (Fig. 3.15). ^{1}H-, ^{13}C-NMR and HSQC spectrum were showed in Table 3.21-3.22 and chemical shifts and coupling constant of HH1 was showed in Figure 3.16. All compounds were described as follows:

Compound HH1: 5-Hydroxy-2-methoxyxanthone

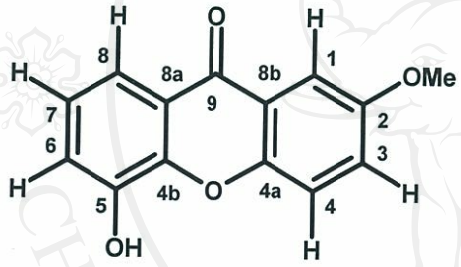

Figure 3.7 The structure of 5-hydroxy-2-methoxyxanthone

Physical appearance: Yellow crystals, mp 247-249°C ($CHCl_3$), mp 245-248°C (Rath *et al.*, 1996)

EI-MS: m/z = 243 [M + H$^+$] ; Molecular formula: $C_{14}H_{10}O_4$

Table 3.5 ^{1}H NMR spectrum ($CDCl_3$, 300 MHz) of 5-hydroxy-2-methoxyxanthone

C/H	δ^{1}H (300 MHz)
H-8	7.88 dd (J=7.8, 1.8)
H-1	7.73 d (J=3.1)
H-4	7.49 d (J=9.1)
H-3	7.36 dd (9.1, 3.1)
H-6	7.34 dd (J=7.8, 1.8)
H-7	7.28 dd (J=7.8, 7.8)
OMe	3.94s (3H)

Table 3.6 COSY spectrum ($CDCl_3$, 300 MHz) of 5-hydroxy-2-methoxyxanthone

δ^1H	shows cross peak with	δ^1H
7.88 dd (J=7.8, 1.8), H-8		7.28 dd (J=7.8, 7.8), H-7
7. 73 d (J=3.1), H-1		7.36 dd (9.1, 3.1), H-3
7.49 d (J=9.1), H-4		7.36 dd (9.1, 3.1), H-3
7.28 dd (J=7.8, 7.8), H-7		7.34 dd (J=7.8, 1.8), H-6

Table 3.7 ^{13}CNMR and HSQC spectrum ($CDCl_3$, 75.47 MHz) of 5-hydroxy-2-methoxyxanthone

$\delta^{13}C$	shows cross peak with	δ^1H
176.92, CO-9		----
156.23, C-2		----
150.22, C-4a		----
144.81, C-5		----
144.68, C-4b		----
124.92, C-3		7.36 dd (9.1, 3.1), H-3
123.80, C-7		7.28 dd (J=7.8, 7.8), H-7
121.98, C-8b		----
121.75, C-8a		----
119.56, C-6		7.34 dd (J=7.8, 1.8), H-6
119.14, C-4		7.49 d (J=9.1), H-4
117.55, C-8		7.88 dd (J=7.8, 1.8), H-8
106.12, C-1		7. 73 d (J=3.1), H-1
55.94, OCH_3		3.94s (3H)

Table 3.8 HMBC spectrum ($CDCl_3$, 500 MHz) of 5-hydroxy-2-methoxyxanthone

δ^1H shows cross peaks with	$\delta^{13}C$
7.88 dd (J=7.8, 1.8), H-8 (**123.85**)	119.56, C-6 144.68, C-4b 176.92, C-9
7. 73 d (J=3.1), H-1 (**106.21**)**1.**	124.92, C-3 150.22, C-4[a]
7.49 d (J=9.1), H-4 (**119.07**)	121.98, C-8b 156.23, C-2
7.34 dd (J=7.8, 1.8), H-6 (**119.49**)	117.56, C-8 144.68, C-4b
7.28 dd (J=7.8, 7.8), H-7 (**123.85**)	121.75, C-8a 144.81, C-5
3.94s, OCH3 (**55.94**)	156.23, C-2

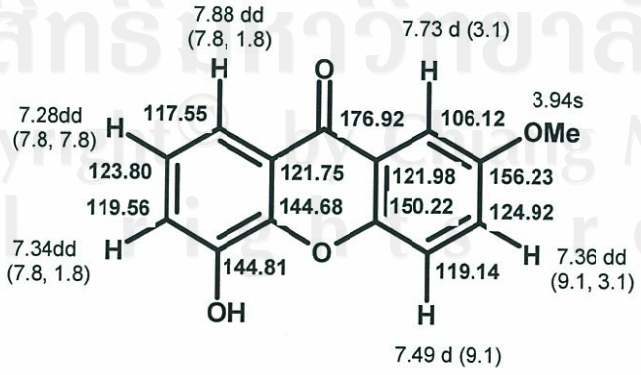

Figure 3.8 Chemical shifts and coupling constant of 5-hydroxy-2-methoxyxanthone

Compound HH2: 2-Hydroxy-3-methoxyxanthone

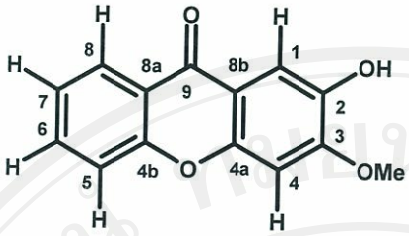

Figure 3.9 The structure of 2-hydroxy-3-methoxyxanthone

Physical appearance: yellow needles, mp 173-175 °C ($CHCl_3$), mp 174-175°C (Gunatilaka *et al.*, 1982)

EI-MS: m/z = 243 [M + H^+] ; Molecular formula: $C_{14}H_{10}O_4$

Table 3.9 ^1H NMR spectrum ($CDCl_3$, 300 MHz) of 2-hydroxy-3-methoxyxanthone

C/H	δ^1H (300 MHz)
H-8	8.33 dd (J=7.9, 1.5)
H-1	7.79 s
H-6	7.69 ddd (J=7.7, 7.7, 1.5)
H-5	7.46 d (J=8.2)
H-7	7.37 dd (J= 7.7, 7.7)
H-4	6.94s
OMe	4.05s (3H)

Table 3.10 ^{13}CNMR and HSQC spectrum ($CDCl_3$, 75.47 MHz) of 2-hydroxy-3-methoxyxanthone

$\delta^{13}C$	shows cross peak with	$\delta^{1}H$
176.26, CO-9		----
156.13, C-4b		----
152.97, C-3		----
151.81, C-2		----
142.98, C-4a		----
134.04, CH-6		7.69 ddd (J=7.7, 7.7, 1.5)
126.59, CH-8		8.33 d (J=7.9, 1.5)
123.71, CH-7		7.37 dd (J= 7.7, 7.7)
121.45, C-8a		----
117.63, CH-5		7.46 d (J=8.2)
115.76, C-8b		----
109.24, CH-1		7.79s
99.11, CH-4		6.94s
56.50, OCH3		4.05s

Table 3.11 HMBC spectrum ($CDCl_3$, 500 MHz) of 5-hydroxy-2-methoxyxanthone

δ^1H	shows cross peaks with	$\delta^{13}C$
8.33 d (J=7.9, 1.5), H-8		176.26 CO-9
(126.59)		156.13 C-4b
		134.04 C-6
7.79s , H-1		176.26 CO-9
(109.24)		152.97 C-3
		142.98 C-4a
7.69 ddd (J=7.7, 7.7, 1.5), H-6		156.13 C-4b
(134.04)		126.59 CH-8
7.46 d (J=8.2), H-5		156.13 C-4b
(117.62)		123.71 C-7
		121.44 C-8a
7.37 dd (J= 7.7, 7.7), H-7		121.44 C-8a
(123.71)		117.63 CH-5
6.94 s, H-4		151.81 C-2
(99.11)		142.98 C-4a
		115.76 C-8b
4.05 s, OMe		152.97 C-3
(56.50)		

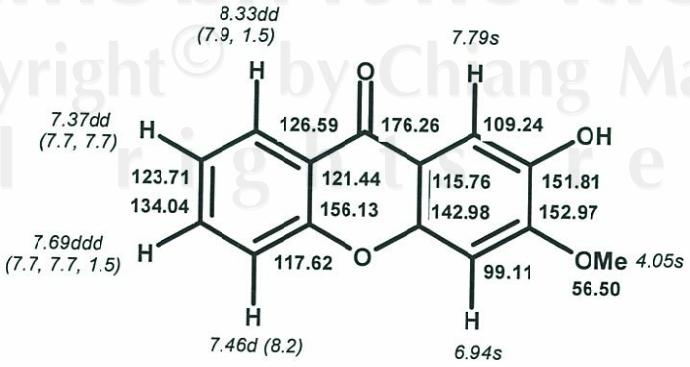

Figure 3.10 Chemical shifts and coupling constant of 5-hydroxy-2-methoxyxanthone

Compounds HH3: *trans*-Kielcorin

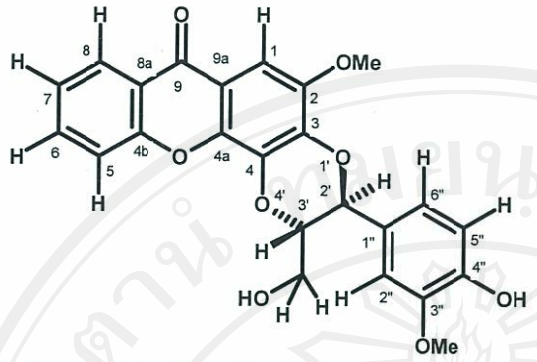

Figure 3.11 The structure of *trans*-Kielcorin

Physical appearance: White crystal, mp 248-250 °C ($CHCl_3$), mp 250-251 °C (Pinto *et al.*, 1987)

FAB-HR-MS: m/z = 437.12370[M + H^+] ; Molecular formula: $C_{24}H_{20}O_8$

Table 3.12 ^1H NMR spectrum ($CDCl_3$, 300 MHz) of *trans*-Kielcorin

C/H	δ^1H (300 MHz)
H-8	8.37 dd (J=7.9, 1.4)
H-6	7.73 ddd (J=7.8, 7.8, 1.6)
H-5	7.59 d (J=8.4)
H-7	7.40 dd (J=7.8, 7.8)
H-1	7.39 s
H-6"	7.01 dd (J=8.0, 2.0)
H-5"	6.98 d (J=7.9)
H-2"	6.98 d (J=2.0)
OH-4"	5.83 brs
H-2'	5.14 d (J=8.1)
H-3'	4.15-4.19 m
CH_2	4.04 dd (J=13.2, 2.1)
	3.68 brd (J=13.2)
OCH_3	3.97s (3H)
OCH_3	3.94s (3H)

Table 3.13 COSY spectrum ($CDCl_3$, 300 MHz) of *trans*-Kielcorin

δ^1H	shows cross peaks with	δ^1H
8.37 dd (J=7.9, 1.4), H-8		7.40 dd (J=7.8, 7.8), H-7
		7.73 ddd (J=7.8, 7.8, 1.6),H-6
7.73 ddd (J=7.8, 7.8, 1.6),H-6		7.59 d (J=8.4), H-5
		7.40 dd (J=7.8, 7.8), H-7
7.01 dd (J=8.0, 2.0), H-6"		6.98 d (J=7.9), H-5"
4.15-4.19 m, H-3'		5.14 d (J=8.1), H-2'
		3.68 brd (J=13.2)
		4.04 dd (J=13.2, 2.1), CH_2
4.04 dd (J=13.2, 2.1), CH_2		3.68 brd (J=13.2), CH_2
		4.15-4.19 m, H-3'

Table 3.14 ^{13}CNMR and HSQC spectrum ($CDCl_3$, 75.47 MHz) of *trans*-Kielcorin

$\delta^{13}C$	**shows cross peak with**	$\delta^{1}H$
176.17 CO-9		----
155.94 C-4b		----
147.01 C-3"		----
146.72 C-4"		----
146.14 C-2		----
141.90 C-4a		----
139.70 C-3		----
134.15 CH-6		7.73 ddd (J=7.8, 7.8, 1.6),H-6
132.40 C-4		----
126.88 C-1"		---
126.61 CH-8		8.37 dd (J=7.9, 1.4), H-8
123.95 CH-7		7.40 dd (J=7.8, 7.8), H-7
121.46 C-8a		----
121.12 CH-6"		7.01 dd (J=8.0, 2.0), H-6"
117.99 CH-5		7.59 d (J=8.4), H-5
114.96 C-9a		----
114.81 CH-5"		6.98 d (J=7.9), H-5"
109.85 CH-2"		6.98 d (J=2.0)
97.56 CH-1		7.39s, H-1
78.28 CH-3'		4.15-4.19 m
77.22 CH-2'		5.14 d (J=8.1)
61.42 CH_2		4.04 dd (J=13.2, 2.1); 3.68 brs (J=13.2)
56.42 OCH_3-2		3.97s
56.12 OCH_3-3"		3.94s

Table 3.15 HMBC spectrum ($CDCl_3$, 500 MHz) of *trans*-Kielcorin

δ^1H	shows cross peaks with	$\delta^{13}C$
8.37 dd (J=7.9, 1.4), H-8		134.15 C-6
(126.61)		155.94 C-4b
		176.17 CO-9
7.73 ddd (J=7.8, 7.8, 1.6),H-6		155.94 C-4b
		126.61 CH-8
7.59 d (J=8.4), H-5		155.94 C-4b
(117.99)		123.95 CH-7
		121.46 C-8a
7.39 s, H-1		139.07 C-3
(97.56)		141.90 C-4a
		146.14 C-2
		132.40 C-4 (weak)
7.01 dd (J=8.0, 2.0), H-6"		109.85 CH-2"
(121.12)		146.72 C-4"
6.98 d (J=7.9), H-5"		126.88 C-1"
(114.96)		
5.83 brs , OH-4"		146.72, C-4"
		114.81 C-5"
5.14 d(8.1), H-2'		109.85 CH-2"
(77.23)		121.12 C-6"
		126.88 C-1"
3.97s, OCH_3-2		146.14 C-2
(56.42)		
3.94 s, OCH_3-4"		147.01 C-4"
(56.12)		

Table 3.16 NOSY spectrum ($CDCl_3$, 300 MHz) of *trans*-Kielcorin

δ^1H	shows cross peaks with	δ^1H
7.40 dd (J=7.8, 7.8), H-7		8.37 dd (J=7.9, 1.4), H-8
		7.73 ddd (J=7.8, 7.8, 1.6),H-6
4.04 dd (J=13.2, 2.1), CH_2		3.68 brd (J=13.2), CH_2
3.97 s, OCH_3-2		7.39s, H-1
3.94 s, OCH_3-3"		6.98 d (J=2.0), H-1"

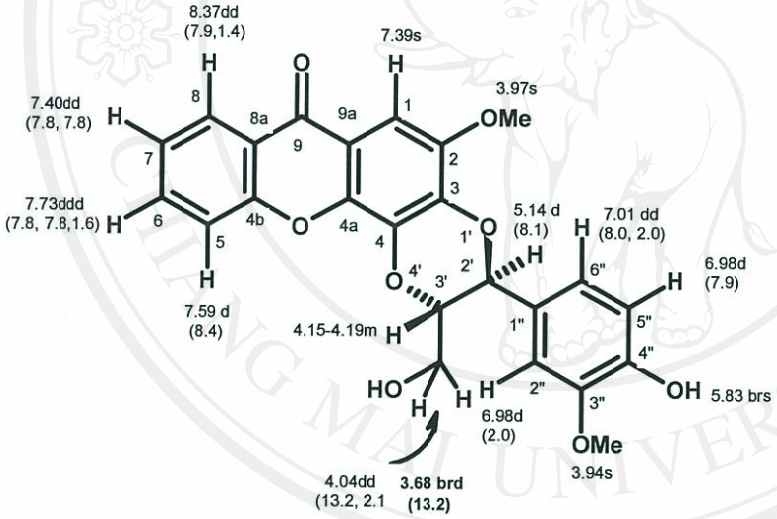

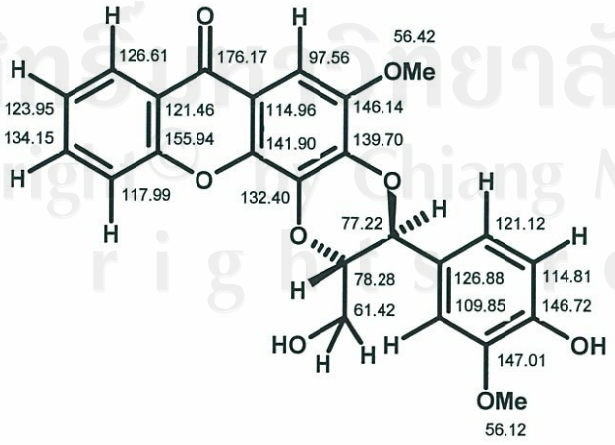

Figure 3.12 Chemical shifts and coupling constant of *trans*-Kielcorin

Compound HH4: 4-Hydroxy-3-methoxyphenyl ferulate

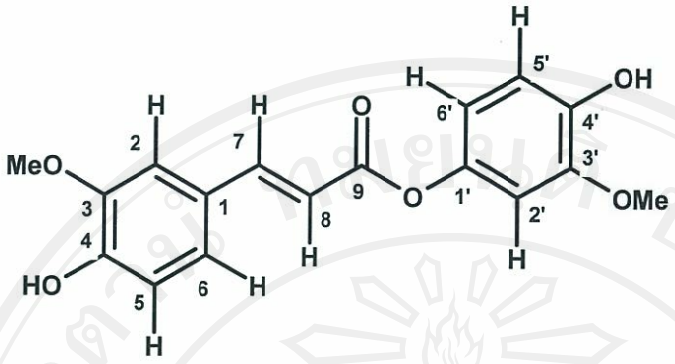

Figure 3.13 The structure of 4-hydroxy-3-methoxyphenyl ferulate

Physical appearance: Yellowish gum

HRMS: m/z = 315.08691 [M - H^+]

Molecular formula: $C_{17}H_{16}O_6$

Table 3.17 ^1H NMR spectrum ($CDCl_3$, 300 MHz) of 4-hydroxy-3-methoxyphenyl ferulate

C/H	δ^1H (300 MHz)
H-7	7.59 d (J=15.9)
H-6	7.07 d (J=8.2)
H-2	7.01s
H-5	6.91d (J=8.2)
H-5'	6.81 d (J=8.2)
H-6'	6.61 d (J=8.0)
H-2'	6.54 s
H-8	6.29 d (J=15.9)
OH-4'	5.93 brs
OH-4	5.52 brs
OCH_3-3	3.92 s (3H)
OCH_3-3'	3.77 s (3H)

Table 3.18 COSY spectrum ($CDCl_3$, 300 MHz) of 4-hydroxy-3-methoxyphenyl-ferulate

δ^1H	shows cross peaks with	δ^1H
7.59 d (J=15.9), H-7		6.29 d (J=15.9), H-8
7.07 d (J=8.2), H-6		6.91d (J=8.2),H-5 7.01s, H-2
6.61 d (J=8.0),H-6'		6.81 d (J=8.2), H-5' 6.54s, H-2'

Table 3.19 ^{13}CNMR and HSQC spectrum ($CDCl_3$, 75.47 MHz) of 4-hydroxy-3-methoxyphenyl ferulate

$\delta^{13}C$	shows cross peak with	δ^1H
167.28 CO-9		----
148.05 C-4		----
146.76 C-3		----
146.43 C-3'		----
145.17 CH-7		7.49 d (J=15.9)
143.87 C-4'		----
131.68 C-1'		----
126.81 C-1		----
123.09 CH-6		7.07 d (J=8.2)
121.71 CH-6'		6.61 d (J=8.0)
115.15 CH-8		6.29 d (J=15.9)
114.72 CH-5		6.91 d (J=8.2)
114.13 CH-5'		6.81 d (J= 8.0)
111.22 CH-2'		6.54s
109.42 CH-2		7.01 s
55.96 OCH_3-3		3.92 s
55.73 OCH_3-3'		3.77 s

Table 3.20 HMBC spectrum ($CDCl_3$, 500 MHz) of 4-hydroxy-3-methoxyphenyl ferulate

δ^1H	shows cross peaks with	$\delta^{13}C$
7.59 d (J=15.9), H-7 (**145.17**)		167.28 CO-9 126.81 C-1 (small) 123.09 CH-6 115.15 CH-8 109. 42 CH-2
7.07 d (J=8.2), H-6 (**123.09**)		148.05 C-4 145.16 CH-7 114.72 CH-5 (small) 109.42 CH-2
7.01s, H-2 (**109.42**)		123.09 CH-6 148.05 C-4 145.16C-7
6.91 d (J=8.2), H-5 (**114.72**)		146.76 C-3 126.81 C-1 123.09 CH-6 (small)
6.81 d (J= 8.0), H-5' (**114.13**)		146.23 C-3' (strong) 143.87 C-4' 131. 68 C-1'
6.61 d (J= 8.0), H-6' (**121.71**)		143.87 C-4' 114.11 CH-5' 111.22 CH-2'
6.54s, H-2' (**111.22**)		146.23 C-3' (weak) 143.87 C-4' (strong) 121.71 CH-6'

Table 3.20 HMBC spectrum ($CDCl_3$, 500 MHz) of 4-Hydroxy-3-methoxyphenyl ferulate (continued)

δ^1H	shows cross peaks with	$\delta^{13}C$
6.29 d (J=15.9), H-8		167.28 CO-9
(**115.15**)		126.81 C-1
5.52 brs (OH-4')		114.11 CH-5'
3.92s, OCH_3-3		146.76 C-3
(**55.96**)		
3.77 s, OCH_3-3'		146.43 C -3'
(**55.73**)		

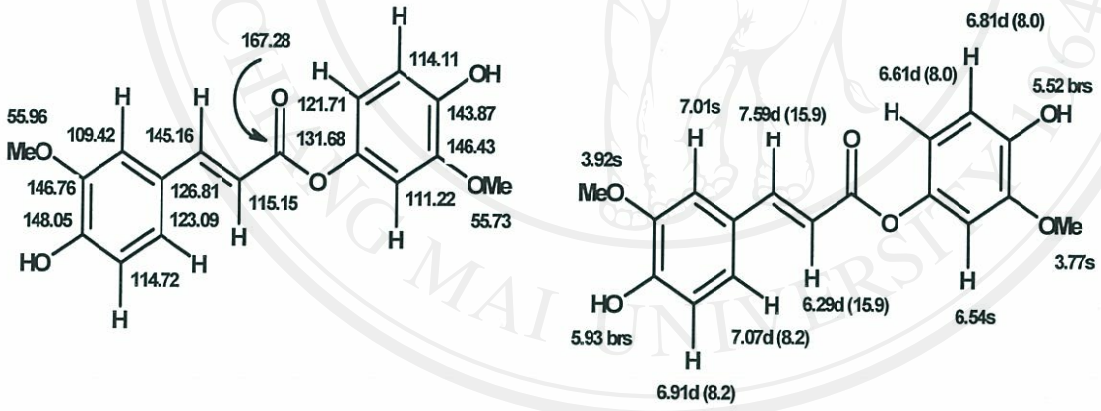

Figure 3.14 Chemical shifts and coupling constant of 4-hydroxy-3-methoxyphenyl ferulate

Compound HH5: 3β-O-caffeoylbetulinic acid

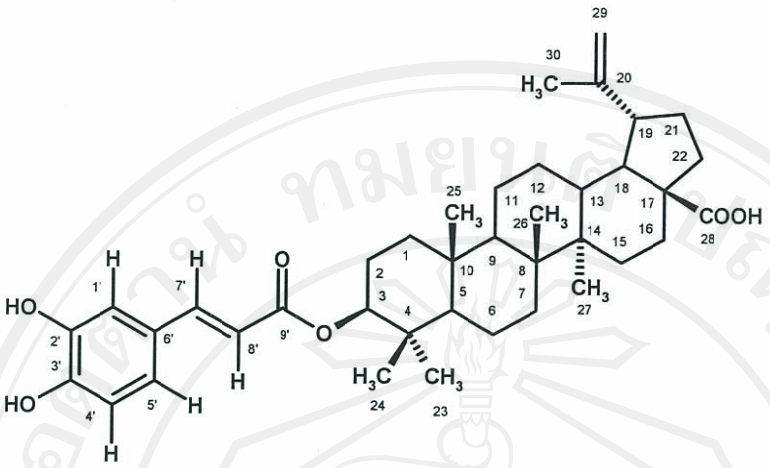

Figure 3.15 The structure of 3β-O-caffeoylbetulinic acid

Physical appearance: colourless solid, m.p.262-264°C ($CHCl_3$), $[\alpha]_D^{30}$ = 138°C

($CHCl_3$, c = 0.145 g/100 ml)

EI-MS: m/z = 617 [M - H^+]

Molecular formula: $C_{39}H_{54}O_6$

Table 3.21 ^{1}H NMR spectrum ($CDCl_3$, 300 MHz) of 3β-O-caffeoylbetulinic acid

C/H	δ^1H (300 MHz)
H-1'	7.08 *brs*
H-4'	6.86 *brd* (J=7.7)
H-5'	6.98 *brd* (J=7.7)
H-7'	7.54 *d* (J=15.8)
H-8'	6.24 *d* (J=15.8)
H-3α	4.62 brs
H-19	2.98-3.01 m
H-29a	4.62 brs
H-29b	4.74 brs
CH_3-23	0.84s (3H)
CH_3-24	0.90s (3H)

Table 3.21 ^{1}H NMR spectrum ($CDCl_3$, 300 MHz) of 3β-O-caffeoylbetulinic acid (continued)

C/H	$\delta^{1}H$ (300 MHz)
CH_3-25	0.88s (3H)
CH_3-26	0.93s (3H)
CH_3-27	0.98s (3H)
CH_3-30	1.62s (3H)

Table 3.22 $^{13}CNMR$ and HSQC spectrum ($CDCl_3$, 75.47 MHz) of 3β-O-caffeoyl betulinic acid

$\delta^{13}C$		shows cross peak with	$\delta^{1}H$
C-1	38.43		----
C-2	22.70		----
C-3	81.12		4.62 brs
C-4	38.06		----
C-5	55.40		----
C-6	18.16		----
C-7	34.20		----
C-8	40.67		----
C-9	50.32		----
C-10	37.13		----
C-11	30.98		----
C-12	25.37		----
C-13	38.06		----
C-14	42.41		----
C-15	21.09		----
C-16	32.16		----
C-17	56.37		----

Table 3.22 ^{13}CNMR and HSQC spectrum ($CDCl_3$, 75.47 MHz) of 3β-O-caffeoyl betulinic acid (continued)

$\delta^{13}C$		shows cross peak with	$\delta^{1}H$
C-18	49.25		-----
C-19	46.97		2.98-3.01m
C-20	150.37		----
C-21	31.93		----
C-22	37.13		----
C-23	28.04		0.84s
C-24	16.20		0.90s
C-25	16.66		0.88s
C-26	16.11		0.93s
C-27	14.68		0.98s
C-28	181.57		----
C-29	109.78		4.62brs; 4.74 brs
C-30	19.35		1.62s
C-1'	114.24		7.08 brs
C-2'	144.61		----
C-3'	146.44		----
C-4'	115.41		6.86d (7.7)
C-5'	122.35		6.98 d (7.7)
C-6'	127.47		----
C-7'	143.99		7.54 d (15.9)
C-8'	116.09		6.24d (15.9)
C-9'	167.68		----

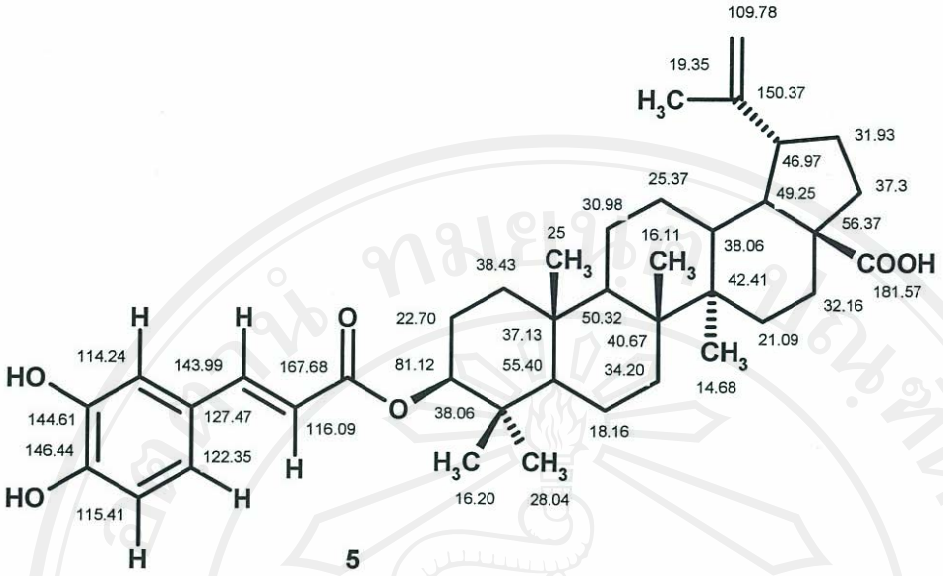

Figure 3.16 Chemical shifts and coupling constant of 3β-O-caffeoylbetulinic acid

Xanthone **HH1** has been reported previously from *Hypericum androsaemum* (Nielson & Arends, 1979), *H. inodorum* (Cardona *et al*., 1992), and *H. roeperanum* (Rath et al., 1996) and xanthone **HH2** from *H. mysorense* (Gunatilaka et al., 1982) while *trans*-kielcorin **HH3** (Pinto *et al*., 1987; Sousa *et al*., 2002), first reported from *Kielmeyera rubriflora* (Gottlieb *et al*., 1971), has subsequently been isolated from a number of *Hypericum* species, inter alia *H. ericoides* (Cardona *et al*., 1982), *H. reflexum* (Cardona *et al*.,1990), and *H. canariensis* (Cardona *et al*., 1986). Information on mp and rotation of caffeate **HH5** from *Betula* species (Ekman et al., 1984; Ohara *et al*., 1986) was not readily accessible; however its ^{1}H and ^{13}C NMR spectra have appeared in the more recent literature (Pan *et al*., 1994; Chen *et al*., 1999). The remaining constituent 4-hydroxy-3-methoxyphenylferulate (**HH4**) has not been described previously.

3.2 Extraction, isolation, purification and structure elucidation of *Schisandra verruculosa*

3.2.1 Preparation of the extract

Dried and powdered stem wood of *S. verruculosa* (10 kg) was percolated by methanol (3 x 20 L) at room temperature. The methanolic solution was evaporated under reduced pressure by a rotary evaporator to give a crude residue (142 g), then dissolved in $CHCl_3$ (3 x 5 L). The $CHCl_3$ solutions were combined and evaporated at reduced pressure to give the chloroform fraction of the methanol extract (118 g).

3.2.2 Chlorophyll elimination of the chloroform extract

Crude $CHCl_3$ fraction of the methanol extract (96 g) was dissolved in warm ethanol (870 ml) to which was added 1 L of hot water containing 34.8 g of lead acetate and 10.4 ml of acetic acid. The solution was kept in a dark chamber for 48 h. The supernatant liquid was filtered, evaporated at reduced pressure to remove ethanol and extracted with chloroform (4 x 250 ml.). The chloroform layer was added with sodium sulfate anhydrous, filtered and evaporated at reduced pressure to give a syrupy mass (4 g).

3.2.3 Fractionation of the extract

The $CHCl_3$ fraction of the methanol extract (4g) was applied to a silica gel column (50 g, 60 x 3 cm) and eluted with Petrol-$CHCl_3$, $CHCl_3$, $CHCl_3$-$(CH_3)_2CO$. Fractions of 300 ml were collected as follows.

Eluents	Fractions
Petrol:$CHCl_3$ (4:1)	1-31
Petrol:$CHCl_3$ (3:2)	32-51

Petrol:$CHCl_3$ (7:3)	52-90
Petrol:$CHCl_3$ (4:1)	91-104
$CHCl_3$	105-123
$CHCl_3$-$(CH_3)_2CO$ (9:1)	124-160
$CHCl_3$-$(CH_3)_2CO$ (7:3)	161-184
$CHCl_3$-$(CH_3)_2CO$ (1:1)	185-197

Fractions were combined according to their composition as revealed by analytical TLC, as follows:

Fractions	**Isolated compounds**
42-56 (227 mg)	not identified
57-72 (180 mg)	**S1** (20 mg)
73-88 (95.5 mg)	not identified
98-108 (125.2 mg)	not identified
109-127 (309.2 mg)	not identified
128-146 (330 mg)	**S2** (12 mg)
147-162 (270 mg)	**S2** (8 mg)
163-170 (223.4 mg)	not identified
171-197 (554.5 mg)	not identified

3.2.4 Isolation and purification of the constituents

Fractions 57-72 (180 mg) were purified by preparative TLC ($C_6H_5CH_3$-$CH_3COOC_2H_5$ -$CHCl_3$-HCO_2H, 50:35:15:1) to give **S1** (20 mg).

Fractions 128-146 (330 mg) were purified by preparative TLC ($CHCl_3$-$(CH_3)_2CO$-HCO_2H, 85:15:1) to give **S2** (12 mg).

Fractions 147-162 (270 mg) were purified by preparative TLC ($CHCl_3$-$(CH_3)_2CO$-HCO_2H, 85:15:1) to give **S2** (8 mg).

3.2.5 Fractionation of the crude extract

Another part of the crude $CHCl_3$ extract (22 g) was applied to silica gel column (200 g, 90 x 4.5 cm) and eluted with Petrol-$CHCl_3$, $CHCl_3$, $CHCl_3$-$(CH_3)_2CO$. Fractions of 500 ml were collected as follows:

Eluents	**Fractions**
Petrol:$CHCl_3$ (7:3)	1-5
Petrol:$CHCl_3$ (1:1)	6-75
Petrol:$CHCl_3$ (3:7)	76-130
Petrol:$CHCl_3$ (1:9)	131-150
$CHCl_3$-$(CH_3)_2CO$ (9:1)	151-165
$CHCl_3$-$(CH_3)_2CO$ (7:3)	166-180

Fractions were combined according to their composition as revealed by analytical TLC, as follows:

Fractions	**Isolated compounds**
1-6 (7.0 g)	not identified
7-30 (857 mg)	small column
31-35 (25.6 mg)	not identified
36-40 (342 mg)	small column
41-45 (21.5 mg)	not identified
46-50 (157 mg)	not identified
51-60 (304.1 mg)	not identified

61-97 (560 mg)	small column
98-130 (0.8 g)	not identified
131-160 (545 mg)	small column
161- 167 (1.2 g)	not identified
168-180 (575.7 mg)	not identified

3.2.6 Isolation and purification of the constituents

Fraction 7- 30 (857 mg) were combined placed on a silica gel column (20 g, 40 x 3 cm), and eluted with Petrol-$CHCl_3$, 100 ml subfractions being collected as follows:

Eluents	**Subfractions**
$CHCl_3$-Petrol (1:1)	1-31
$CHCl_3$-Petro (7:3)	32-53
$CHCl_3$-Petro (9:1)	55-65

Subfractions were combined according to their composition as revealed by analytical TLC, as follows:

Subfractions	**Isolated compounds**
1-4 (195.4 mg)	not purified
5-8 (23 mg)	**S3** (3.3 mg)
	S4 (6.9 mg)
9-15 (24 mg)	**S4** (8.3 mg)
16-20 (55.1 mg)	not purified
21-30 (33.4 mg)	not purified
31-40 (44.2 mg)	not purified

41-50 (11.8 mg)	not purified
51-55 (9.2 mg)	not purified
56-65 (19.1 mg)	not purified

Subfractions 5-8 (23 mg) were purified by preparative TLC ($CHCl_3$-Petrol-HCO_2H, 95:5:1) to give **S3** (3.3 mg) and **S4** (6.9 mg).

Subfractions 9-15 (24 mg) were purified by preparative TLC ($CHCl_3$-Petrol-HCO_2H, 95:5:1) to give **S4** (8.3 mg).

Fraction 36-40 (342 mg), were combined and chromatographed over silica gel column (15 g, 30 x 2.5 cm), and eluted with Petrol-$CHCl_3$, 100 ml subfractions being collected as follows:

Eluents	**Subfractions**
$CHCl_3$-Petrol (1:1)	1-50
$CHCl_3$-Petrol (7:3)	51-55
$CHCl_3$-Petrol (9:1)	56-65

Subfractions were combined according to their composition as revealed by analytical TLC, as follows:

Fractions	**Isolated compounds**
1-4 (28.6 mg)	not purified
5-11 (42 mg)	**S5** (23 mg)
	S6 (9.6 mg)
12-15 (24.2 mg)	not purified
16-20 (27.2 mg)	not purified
21-30 (35.7 mg)	not purified

31-40 (43.6 mg)	not purified
41-55 (17.4 mg)	not purified
56-65 (12.8 mg)	not purified

Subfractions 5-11 (42 mg) were purified by preparative TLC ($CHCl_3$-$(CH_3)_2CO$-HCO_2H, 85:15:0.1%) to give **S5** (23 mg) and **S6** (9.6 mg).

Fractions 61-97 (560 mg) were combined, chromatographed over silica gel column (15 g, 40 x 2.5 cm), and eluted with $CHCl_3$-Petrol, 100 ml subfractions being collected as follows:

Eluents	**Subfractions**
$CHCl_3$-Petrol (1:1)	1-47
$CHCl_3$-Petro (7:3)	48-73

Subractions were combined according to their composition as revealed by analytical TLC, as follows:

Subfractions	**Isolated compounds**
1-10 (134.2 mg)	not purified
11-20 (93.7 mg)	not purified
21-40 (69 mg)	**S5** (11 mg)
	S7 (9.5 mg)
41-46 (29.9 mg)	not purified
47-52 (17.9 mg)	not purified
53-63 (72.3 mg)	not purified
64-73 (20.2 mg)	not purified

Subfractions 21-40 (69 mg) were purified by preparative TLC ($CHCl_3$: $(CH_3)_2CO$: HCO_2H, 85:15:1) to give **S5** (11 mg) and **S7** (9.5 mg)

Fraction 131- 160 (545 mg) were combined, chromatographed over silica gel column (15 g, 30 x 2.5 cm), and eluted with $CHCl_3$-Petrol, 200 ml subfractions being collected as follows:

Eluents	**Subfractions**
$CHCl_3$-Petrol (7:3)	1-22
$CHCl_3$-Petro (9:1)	23-34
$CHCl_3$-$(CH_3)_2CO$ (9:1)	35-40
$CHCl_3$-$(CH_3)_2CO$ (7:3)	41-50

Subfractions were combined according to their composition as revealed by analytical TLC, as follows:

Subfractions	**Isolated compounds**
1-10 (342.3 mg)	not purified
11-15 (69.4 mg)	not purified
16-23 (89.9 mg)	not purified
24-35 (74 mg)	**S8** (15 mg)
36-39 (23.9 mg)	not purified
40-50 (48.4 mg)	not purified

Subfractions 24-35 (74 mg) were purified by preparative TLC ($CHCl_3$-MeOH-HCO_2H, 96:4:1) to give **S8** (15 mg).

3.2.7 Stucture elucidation

Compounds S1-S8 were elucidated for their structure by ^{1}H-, ^{13}C-NMR, mass spectrometry, COSY and HMBC.

S1 was identified as 4 hydroxy-3-methoxy benzoic acid (vanillic acid) (Fig. 3.17). ^{1}H-, ^{13}C-NMR, HSQC and HMBC spectra were shown in Table 3.23-3.25.

S2 was identified as abscisic acid (Fig. 3.118). ^{1}H-, ^{13}C-NMR and HSQC spectrum were showed in Table 3.26-3.27.

S3 was identified as methyl 4-hydroxybenzoate (Fig. 3.19). ^{1}H-, ^{13}C-NMR, HSQC and HMBC spectra were shown in Table 3.28-3.30.

S4 was identified as 4 hydroxybenzaldehyde (Fig. 3.20). ^{1}H-, ^{13}C-NMR, COSY, HSQC and HMBC spectra were shown in Table 3.31-3.34.

S5 was identified as methyl 3,4-dihydroxybenzoate (Fig. 3.21). ^{1}H-, ^{13}C-NMR, COSY, HSQC and HMBC spectra were shown in Table 3.35-3.38.

S6 was identified as 1-(4-hydroxy-3-methoxyphenyl)-3-hydroxypropan-1-one (Fig. 3.22). ^{1}H-, ^{13}C-NMR, COSY, COSY, HSQC and HMBC spectra were shown in Table 3.39-3.42.

S7 was identified as 1,2-bis (4- hydroxy-3-methoxyphenyl)-3-hydroxypropan-1-one (evafolin B) (Fig. 3.23). ^{1}H-, ^{13}C-NMR, HSQC and HMBC spectra were shown in Table 3.43-3.46.

S8 was identified as 4 hydroxybenzoic acid (Fig. 3.24). ^{1}H-, ^{13}C-NMR and HSQC spectra were shown in Table 3.47-3.48.

All compounds were described as follows:

Compound S1: 4 Hydroxy-3-methoxybenzoic acid (Vanillic acid)

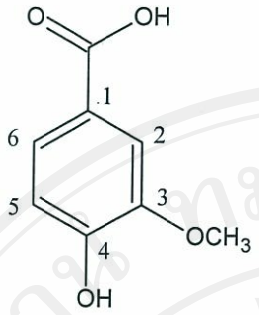

Figure 3.17 The structure of vanillic acid

Physical appearance: Yellow liquid.

Molecular formula: $C_8H_8O_4$

Table 3.23 ^{1}H NMR spectrum ($CDCl_3$, 300 MHz) of vanillic acid

C/H	**δ^1H (300 MHz)**
COOH	9.9 brs
H-6	7.43 dd (J=8.0,1.6)
H-2	7.42 s
H-5	6.83 d (J=8.0)
OCH_3	3.97s (3H)

Table 3.24 ^{13}CNMR and HSQC spectrum ($CDCl_3$, 75.47 MHz) of vanillic acid

$\delta^{13}C$	shows cross peak with	$\delta^{1}H$
167.35, COO		----
151.12, C-4		----
147.27, C-3		----
123.54, C-6		7.43 dd (J=8.0,1.6), H-6
121.69, C-1		----
115.07, C-5		6.83 d (J=8.0), H-5
112.71, C-2		7.42 s, H-2
55.58, OCH_3		3.97s (3H)

Table 3.25 HMBC spectrum ($CDCl_3$, 300 MHz) of vanillic acid

$\delta^{1}H$	shows cross peaks with	$\delta^{13}C$
7.43 dd (J=8.0,1.6), H-6		112.71 C-2
(**123.54**)		151.12 C-4
		167.35 COO
7.42 s, H-2		123.54 C-6
(**112.71**)		151.12 C-4
		167.35 COO
6.83 d (J=8.0), H-5		121.69 C-1
(**115.07**)		147.27 C-3

Compound S2: Abscisic acid

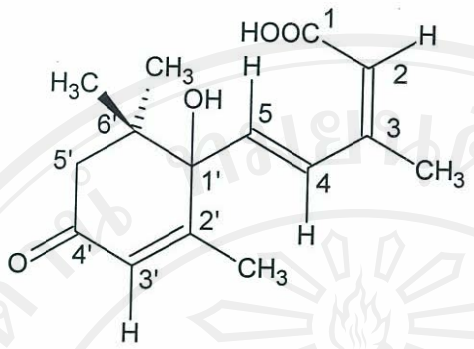

Figure 3.18 The structure of abscisic acid

Molecular formula: $C_{15}H_{20}O_4$

Table 3.26 ^{1}H NMR spectrum ($CDCl_3$, 300 MHz) of abscisic acid

C/H	δ^1H (300 MHz)
COOH	9.9 brs
H-4	7.38 d (J=16.0)
H-5	6.16 d (J=16.0)
H-3'	5.96 brs
H-2	5.78 brs
H-5'	2.49 d (J=17.0)
	2.30 d (J=17.0)
Me-3	2.40 d (J=1.0) (3H)
Me-2'	1.93 d (J=1.2) (3H)
Me-6'	1.12 s (3H)
	1.03 s (3H)

Table 3.27 ^{13}CNMR and HSQC spectrum ($CDCl_3$, 75.47 MHz) of abscisic acid

$\delta^{13}C$	shows cross peak with	$\delta^{1}H$
197.98, C-4'		----
170.31, C-1		----
162.58, C-2'		----
151.57, C-3'		----
136.93, C-5		----
128.12, C-4		----
117.83, C-2		----
79.80, C-1		----
49.68, C-5'		----
41.58, C-6'		----
24.31, Me-6'		----
23.80, Me-6'		----
21.44, Me-3		----
18.98, Me-2'		----

Compound S3: Methyl 4-hydroxybenzoate

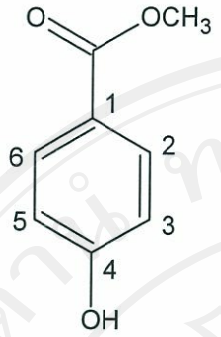

Figure 3.19 The structure of methyl 4-hydroxybenzoate

Molecular formula: $C_8H_8O_3$

Table 3.28 ^{1}H NMR spectrum ($CDCl_3$, 300 MHz) of methyl 4-hydroxybenzoate

C/H	**δ^1H (300 MHz)**
H-2, H-6	7.96 d (J=8.5)
H-5, H-3	6.86 d (J=8.5)
OMe	3.88 s (3H)

Table 3.29 ^{13}CNMR and HSQC spectrum ($CDCl_3$, 75.47 MHz) of methyl 4-hydroxy benzoate

δ^{13}C shows cross peak with	**δ^1H**
166.80, COO	----
159.64, C-4	----
131.89, C-2, C-6	7.96 d (J=8.5), H-2, H-6
122.86, C-1	----
115.14, C-3, C-5	6.86 d (J=8.5), H-3, H-5
51.92, OCH_3	3.88 s (3H)

Table 3.30 HMBC spectrum ($CDCl_3$, 500 MHz) of methyl 4-hydroxybenzoate

δ^1H	**shows cross peaks with**	$\delta^{13}C$
7.96 d (J=8.5), H-2, H-6		115.14 C-3, C-5
(**131.89**)		131.89 C-2, C-6
		159.64 C-4
		166.80 COO
6.86 d (J=8.5), H-3, H-5		115.14 C-3, C-5
(**115.14**)		122.86 C-1

Compound S4: 4-Hydroxybenzaldehyde

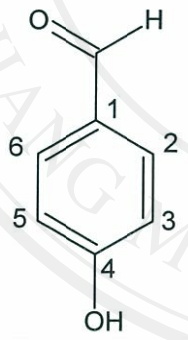

Figure 3.20 The structure of 4-Hydroxybenzaldehyde

Molecular formula: $C_7H_6O_2$

Table 3.31 ^1H NMR spectrum ($CDCl_3$, 300 MHz) of 4-hydroxybenzaldehyde

C/H	**δ^1H (300 MHz)**
CHO	9.79 s
H-2, H-6	7.74 d (J=8.5)
H-5, H-3	6.89 d (J=8.5)

Table 3.32 COSY spectrum ($CDCl_3$, 300 MHz) of 4-hydroxybenzaldehyde

δ^1H	shows cross peaks with	δ^1H
7.74 d (J=8.5, 6.8), H-2, H-6		6.89 d (J=8.5), H-3, H-5

Table 3.33 $^{13}CNMR$ and HSQC spectrum ($CDCl_3$, 75.47 MHz) of 4-hydroxybenzal dehyde

$\delta^{13}C$	shows cross peak with	δ^1H
190.99 COH		----
161.57 C-4		----
132.40 C-6		7.74 d (J=8.5), H-2, H-6
129.84 C-1		----
115.94 C-3, C-5		6.89 d (J=8.5), H3, H-5

Table 3.34 HMBC spectrum ($CDCl_3$, 500 MHz) of 4-hydroxybenzaldehyde

δ^1H	shows cross peaks with	$\delta^{13}C$
9.79 s, CHO		129.84 C-1
(**190.99**)		132.40 C-2, C-6
7.74 d (J=8.5)H-2, H-6		132.40 C-2, C-6
(**132.40**)		161.51 C-4
		190.99 CHO
6.89 d (J=8.5), H3,H-5		115.94 C-3, C-5
(115.94)		129.87 C-1
		161.57 C-4

Compound S5: Methyl 3,4-dihydroxybenzoate

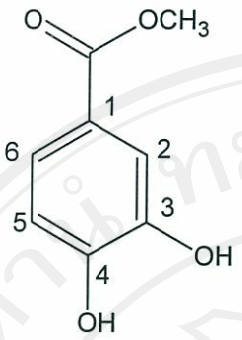

Figure 3.21 The structure of methyl 3,4-dihydroxybenzoate

Physical appearance: White solid

Molecular formula: $C_8H_8O_4$

Table 3.35 ^{1}H NMR spectrum ($CDCl_3$, 500 MHz) of methyl 3,4-dihydroxybenzoate

C/H	**δ^1H (500 MHz)**
H-2	7.59 d (J=2.0)
H-6	7.56 dd (8.2,2.0)
H-5	6.91 d (J=8.2)
OCH_3	3.88s (3H)

Table 3.36 COSY spectrum ($CDCl_3$, 300 MHz) of methyl 3,4-dihydroxybenzoate

δ^1H	**shows cross peaks with**	**δ^1H**
7.56 dd (J=8.2, 2.0), H-6		6.91 d (J=8.2), H-5

Table 3.37 ^{13}CNMR and HSQC spectrum ($CDCl_3$, 75.47 MHz) of methyl 3,4-dihydroxy benzoate

$\delta^{13}C$	**shows cross peak with**	**$\delta^{1}H$**
167.08	COO	----
148.71	C-4	----
143.13	C-3	----
123.67	C-6	7.56 dd (J=8.2,2.0)H-6
122.53	C-1	----
116.49	C-2	7.59 d (J=2.0), H-2
114.77	C-5	6.91 d (J=8.2), H-5
52.04	OCH_3	3.88s (3H)

Table 3.38 HMBC spectrum ($CDCl_3$, 300 MHz) of methyl 3,4-dihydroxybenzoate

$\delta^{1}H$	**shows cross peaks with**	**$\delta^{13}C$**
7.59 d (J=2.0), H-2		123.67 C-6
(116.49)		148.71 C-4
		167.08 COO
7.56 dd (8.2,2.0),H-6		116.49, C-2
(123.67)		148.71 C-4
		167.08 COO
6.91 d (J=8.2), H-5		122.53 C-1
(114.77)		143.13 C-3

Compound S6: 1-(4-Hydroxy-3-methoxyphenyl)-3-hydroxy-propan-1-one

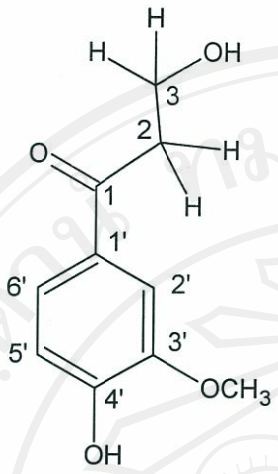

Figure 3.22 The structure of 1-(4-hydroxy-3-methoxyphenyl)-3-hydroxy-propan-1-one

Physical appearance: Yellow liquid; $[\alpha]_D^{25}$ = -16 ° ($CHCl_3$, c=1.2g/100 ml)

Molecular formula: $C_{10}H_{12}O_4$

Table 3.39 ^1H NMR spectrum ($CDCl_3$, 300 MHz) of 1-(4-hydroxy-3-methoxy phenyl)-3- hydroxy-propan-1-one

C/H	**δ^1H (300 MHz)**
H-6'	7.57 d (J=7.8)
H-2'	7.54 s
H-5'	6.96d (J=7.8)
OH-4	6.14 brs
H-3	4.03t (J=5.3) (2H)
OCH_3	3.97 s (3H)
H-2	3.19t (J=5.3) (2H)

Table 3.40 COSY spectrum ($CDCl_3$, 300 MHz) of 1-(4-hydroxy-3-methoxyphenyl)-3-hydroxy-propan-1-one

δ^1H	shows cross peaks with	δ^1H
7.55 dd (J=8.4, 1.6), H-6'		6.96d (J=7.8), H-5'
4.03t (j=5.3), H-3'		3.19t (J=5.3), H-2'

Table 3.41 ^{13}CNMR and HSQC spectrum ($CDCl_3$, 125.77 MHz) of 1-(4-hydroxy-3-methoxyphenyl)-3-hydroxy-propan-1-one

$\delta^{13}C$	shows cross peak with	δ^1H
199.10 CO-1		----
150.77 C-4'		----
146.66 C-3		----
129.60 C-1'		----
123.66 C-6'		7.57 d (J=7.8), H-6'
113.92 C-5'		6.96 d (J=7.8), H-5'
109.51 C-2'		7.54s
58.32 C-3		4.03t (J=5.3)
56.08 OCH_3		3.97 s
39.73 C-2		3.19t (J=5.3)

Table 3.42 HMBC spectrum ($CDCl_3$, 500 MHz) of 1-(4-hydroxy-3-methoxyphenyl)-3-hydroxy-propan-1-one

δ^1H	shows cross peaks with	$\delta^{13}C$
7.57 d (J=7.8), H-6'		109.51 C-2
(123.66)		150.77 C-4
		199.10 CO-1
7.54s, H-2		123.66 C-6
(109.51)		150.77 C-4
		199.10 CHO
6.96d (J=7.8), H-5		129.60 C-1
(113.92)		146.66 C-3
3.97s, OMe		146.66 C-3'
(56.08)		
4.03 t (J=5.3), H-3		39.73 C-2
(58.32)		199.10 CO-1
3.19t (J=5.3), H-2		58.32 C-3
(39.73)		199.10 CO-1

Compound S7: 1,2-bis(4-hydroxy-3-methoxyphenyl)-3-hydroxy-propan-1-one

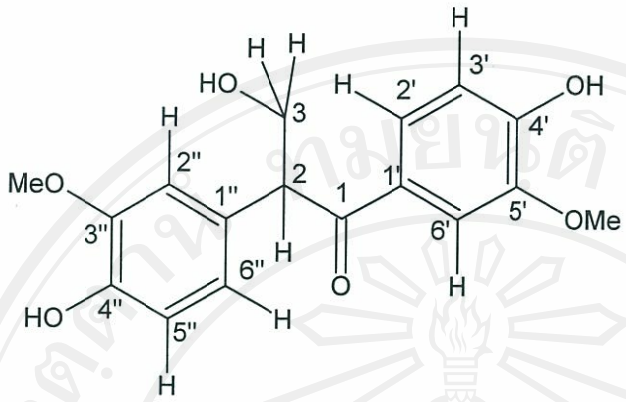

Figure 3.23 The structure of 1,2-bis- (4-hydroxy-3-methoxyphenyl)-3-hydroxy-propan-1-one

Physical appearance: white viscous mass, $[\alpha]_D^{25} = -16^{\circ}$ ($CHCl_3$, c = 1.2g/100 mL)

EI-HRMS: M^+ 318.11028 ; Molecular formula: $C_{17}H_{18}O_6$

Table 3.43 ^1H NMR spectrum ($CDCl_3$, 300 MHz) of 1,2-bis- (4-hydroxy-3-methoxy phenyl) -3-hydroxy-propan-1-one

C/H	δ^1H (300 MHz)
H-2'	7.54 d (1.9)
H-6'	7.53 dd (J=8.8, 1.9)
H-5"	6.86d (J=8.0)
H-5'	6.84 d (J=8.8)
H-6"	6.80dd (8.0, 1.9)
H-2"	6.71d (J=1.9)
H-2	4.66 dd (8.2, 5.0)
H-3	4.22 dd (J=11.3, 8.4) (2H)
H-3	3.82-3.89 m
OMe-3"	3.90s (3H)
OMe-5'	3.84s (3H)

Table 3.44 COSY spectrum ($CDCl_3$, 300 MHz) of 1,2-bis-(4-hydroxy-3-methoxy-phenyl)-3-hydroxy-propan-1-one

δ^1H	shows cross peaks with	δ^1H
4.66 dd (8.2, 5.0), H-2		4.22 dd (J=11.3, 8.4), H-3 3.82-3.89m, H-3
4.22 dd (J=11.3, 8.4), H-3		3.82-3.89m, H-3 4.66 dd (8.2, 5.0), H-2

Table 3.45 ^{13}CNMR and HSQC spectrum ($CDCl_3$, 125.77 MHz) of 1,2-bis(4-hydroxy -3-methoxyphenyl)-3-hydroxy-propan-1-one

$\delta^{13}C$	shows cross peak with	δ^1H
198.58CO-1		----
150.51C-4'		----
146.94C-3"		----
146.48C-3'		----
145.07 C-4"		----
129.06 C-1'		----
128.43 C-1"		----
124.45 CH-6'		7.53 dd (J=8.8, 1.9)
121.54 CH-6"		6.80 dd (8.0, 1.9)
114.95 CH-5"		6.86 d (J=8.0)
113.89 CH-5'		6.84 d (J=8.8)
110.53 CH-2'		7.54 d (1.9)
110.09 CH-2"		6.71d (J=1.9)
65.29 CH_2-3		4.22 dd (J=11.3, 8.4); 3.82-3.89 m
55.94 OMe		3.90s and 3.84s
55.47 CH-2		4.66 dd (8.2, 5.0)

Table 3.46 HMBC spectrum ($CDCl_3$, 300 MHz) of 1,2-bis- (4-hydroxy-3-methoxy-phenyl)-3-hydroxy-propan-1-one

δ^1H	shows cross peaks with	$\delta^{13}C$
3.82-3.89 m, H-3		128.43 C-1”
(65.29)		198.58 C-1 (strong)
4.22 dd (J=11.3, 8.4); H-3		198.58 C-1 (weak)
(65.29)		
4.66 dd (8.2, 5.0), H-2		65.29 C-3
		110.09C-2”
		121.54 C-6”
		128.43 C-1”
		198.58 CO-1
6.71d (J=1.9), H-2”		55.47 CH-2
(110.09)		121.54 CH-6”
		145.07 C-4”
		146.94 C-3”
6.80 dd (8.0, 1.9), H-6”		110.90 CH-2”
(121.54)		145.07 C-4”
6.84 d (J=8.8), H-5’		129.06 C-1’
(113.89)		1146.94 C-3’
		150.51 C-4’
6.86 d (J=8.0), H-5”		128.43 C-1”
(114.95)		146.48 C3”
7.53 dd (J=8.8, 1.9), H-6’/ 7.54 d (1.9), H-2’		110.53 CH-2’
(124.45)/(110.53)		124.45 CH-6’
		129.06 C-1’
		146.48 C-3’
		150.51 C-4’

Compound S8: 4-Hydroxybenzoic acid

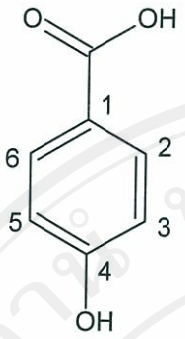

Figure 3.24 The structure of 4-hydroxybenzoic acid

Molecular formula: $C_7H_6O_3$

Table 3.47 ^{1}H NMR spectrum ($CDCl_3$, 300 MHz) of 4-hydroxybenzoic acid

C/H	δ^1H (300 MHz)
H-2, H-6	7.79 d (J=8.5)
H-5, H-3	6.80 d (J=8.5)

Table 3.48 ^{13}CNMR and HSQC spectrum ($CDCl_3$, 75.47 MHz) of 4-hydroxybenzoic acid

δ^{13}C	shows cross peak with	δ^1H
167.17 COO		----
161.44 C-4		----
131.29 C-2, C-6		7.79 d (J=8.5), H-2, H-6
121.26 C-1		6.80 d (J=8.5), H-5, H-3
114.83 C-3, C-5		----

In spite of lignans, common plant secondary metabolites were isolated from the stem wood of *Schisandra verruculosa*. Though compounds **S6** and **S7** were isolated for the first time from the plants of the genus *Schisandra*, they have been previously reported as constituents of *Bauhenia manca* (Achenbach *et al.*, 1988) and *Tetradium glabrifolium* (Wu *et al.*, 1995), respectively.

Part 4: Bioactivities of the isolated compounds

4.1 Tumor cell growth assay

The effect of compounds from *H. hookerianum* on the *in vitro* growth of MCF-7, NCI-H460, SF-268, and UACC-62 cell lines, given in concentration that were able to cause 50% of cell growth inhibition (GI_{50}) after a continuous exposure of 48 h, is shown in Table 3.49 (calculation data are in appendix D). All the compounds exhibited a dose dependent growth inhibitory effect against all the tumor cell lines tested. Compounds **HH4** and **HH5** exhibited stronger growth inhibitory effects than compounds **HH1** and **HH2** While the formers exhibited activities of the same magnitude, compounds **HH1** and **HH2** showed to be more active against UACC-62.

The effect of **HH3** has also been studied against these cells lines. A moderate effect was detected in our study which is in accordance with that previously described for this compound. (Sousa *et al*., 2002).

Table 3.49 The GI_{50} of compounds from *Hypericum hookerianum* on the growth of human cancer cell lines

	GI_{50} (μM)[a]			
Compounds	MCF-7	NCI-H460	SF-268	UACC-62
HH1	98.1 ± 8.5	108.5 ± 15.3	134.3 ± 9.9	49.6 ± 0
HH2	100 ± 17.5	178.7 ± 17.2	144.6± 25.8	67.5 ± 1.4
HH3	55.1 ± 2.3	49.7 ± 3.0	40.5 ± 1.5	ND
HH4	15.1 ± 1.6	18.7 ± 2.3	15.9 ± 2.7	21.2 ± 0.7
HH5	12.2 ± 2.4	19.6 ± 2.3	24.3 ± 2.5	31.8 ± 0.5
Doxorubicin[b]	42.8 ± 8.2	94.0 ± 8.7	93.0 ± 7.0	94.0 ± 0.9

[a]Results show means ± SEM of 3-4 independent experiments performed in duplicate.

[a]Data from the positive control doxorubicin are expressed in nM.

Table 3.50 The GI_{50} of compounds from *Shisandra verruculosa* on the growth of human cancer cell lines

Compounds	GI_{50} (μM)[a]		
	MCF-7	NCI-H460	SF-268
S1	174.6 ± 8.5	> 200	> 200
S2	> 189.4	> 189.4	> 189.4
S3	172.7 ± 8.2	176.3 ± 4.4	180.9 ± 5.7
S4	> 200	> 200	> 200
S5	78.9 ± 6.1	38.8 ± 3.3	93.8 ± 7.9
S6	> 200	> 200	> 200
S7	> 157.2	> 157.2	> 157.2
S8	> 200	> 200	> 200
Doxorubicin[b]	42.8 ± 8.2	94.0 ± 8.7	93.0 ± 7.0

[a]Results show means ± SEM of 3-4 independent experiments performed in duplicate.

[a]Data from the positive control doxorubicin are expressed in nM.

The GI_{50} of the compounds isolated from *S. verrucolosa* on MCF-7, NCI-H460 and SF-268 were shown in Table 3.50. From the results, only compounds **S5** exhibited the moderate growth inhibitory effect against three cell lines and to be more active against NCI-H460.

4.2 Human lymphocytes proliferation assay

The effect of compounds from *H. hookerianum* on the mitogenic response of human lymphocytes to PHA, was also studied and the results, given in concentrations that were able to cause 50% inhibition of proliferation (IC_{50}), are shown in Table 3.51 (calculation data are in appendix D). All compounds inhibited in a dose dependent manner the proliferation of lymphocytes. Compounds **HH1** and **HH2** showed once again to be weaker inhibition than compounds **HH4** and **HH5**. **HH3** showed no antiproliferative activity even at the maximum concentration tested. No activity was also found for this **HH3** in a previous study (Sousa *et al.*, 2002).

Table 3.51 The IC_{50} of compounds from *Hypericum hookerianum* on proliferation of human lymphocytes assay

Compounds	IC_{50} (μM)[a]
HH1	168.8 ± 4.1
HH2	171.6 ± 11.7
HH3	> 114.7
HH4	26.1 ± 3.6
HH5	40.8 ± 4.9
Cyclosporin A	0.34 ± 0.04

Results show means ±SEM of 3-4 independent experiments performed in duplicate.

The effect of compounds on the mitogenic response of human lymphocytes to PHA, was also studied with the compound isolated from *S. verrucolosa* and the results, given in concentrations that were able to cause 50% inhibition of proliferation (IC_{50}), are shown in Table 3.52. Compound **S5** showed once again a moderate antiproliferative activity while the other compounds were devoid of activity even at the maximum concentration tested.

Table 3.52 The IC_{50} of compounds from *Shisandra verruculosa* on proliferation of human lymphocytes assay

Compounds	IC_{50} (μM)[a]
S1	> 200
S2	> 189.4
S3	> 200
S4	> 200
S5	58.58 ± 5.6
S6	**> 200**
S7	**> 157.2**
S8	**> 200**
Cyclosporin A	0.34 ± 0.04

Results show means ±SEM of 3-4 independent experiments performed in duplicate.

Neither compounds **HH4** and **HH5** from *H. hookerianum* nor compound **S5** from *S. verrucolosa* showed lymphocytotoxicity when the human lymphocytes were exposed to the maximum concentration tested (99% cell viability) (Calculation data

are in appendix D), which leads to the conclusion that the inhibitory activity was associated with cell proliferation rather than to a toxic effect.

4.3 Free radical scavenging activity

The concentration of isolated compounds from *H. hookerianum* and *S. verruculosa*, which showed 50% DPPH scavenging activity (IC_{50}) were reported in table 3.53 and table 3.54, respectively.

The results showed that compound S5 has a strong scavenging activity for DPPH free radical with IC_{50} value close to the positive control, ascorbic acid. Compounds HH4 and HH5 showed also moderate scavenging activity.

Table 3.53 The IC_{50} of compounds from *Hypericum hookerianum* on DPPH free radical scavenging activity assay

Compounds	IC_{50} (μM)
HH1	> 100
HH2	> 100
HH3	> 100
HH4	48.2 ± 6.1
HH5	15.6 ± 0.8
Ascorbic acid	5.3 ± 0.2

Results show means ±SEM of 3-4 independent experiments performed in triplicate.

Table 3.54 The IC_{50} of compounds from *Shisandra verruculosa* on DPPH free radical scavenging activity assay

Compounds	IC_{50} (μM)
S1	> 100
S2	> 100
S3	> 100
S4	> 100
S5	6.4 ± 0.2
S6	> 100
S7	> 100
S8	> 100
Ascorbic acid	5.3 ± 0.2

Results show means ±SEM of 3-4 independent experiments performed in triplicate.